SEDIMENTOLOGY the journal of the International Association of Sedimentologists

Sedimentology (2018) doi: 10.1111/sed.12438

Expanding the spectrum of shallow-marine, mixed carbonate–siliciclastic systems: Processes, facies distribution and depositional controls of a siliciclastic-dominated example

ERNESTO SCHWARZ, GONZALO D. VEIGA, GASTÓN ÁLVAREZ TRENTINI, MANUEL F. ISLA and LUIS A. SPALLETTI
Centro de Investigaciones Geológicas (Universidad Nacional de La Plata-CONICET), Diagonal 113 #256, B1904DPK, La Plata, Argentina (E-mail: eschwarz@cig.museo.unlp.edu.ar)

Associate Editor – Christopher Fielding

ABSTRACT

Most of the present knowledge of shallow-marine, mixed carbonate–siliciclastic systems relies on examples from the carbonate-dominated end of the carbonate–siliciclastic spectrum. This contribution provides a detailed reconstruction of a siliciclastic-dominated mixed system (Pilmatué Member of the Agrio Formation, Neuquén Basin, Argentina) that explores the variability of depositional models and resulting stratigraphic units within these systems. The Pilmatué Member regressive system comprises a storm-dominated, shoreface to basinal setting with three subparallel zones: a distal mixed zone, a middle siliciclastic zone and a proximal mixed zone. In the latter, a significant proportion of ooids and bioclasts were mixed with terrigenous sediment, supplied mostly via along-shore currents. Storm-generated flows were the primary processes exporting fine sand and mud to the middle zone, but were ineffective to remove coarser sediment. The distal zone received low volumes of siliciclastic mud, which mixed with planktonic-derived carbonate material. Successive events of shoreline progradation and retrogradation of the Pilmatué system generated up to 17 parasequences, which are bounded by shell beds associated with transgressive surfaces. The facies distribution and resulting genetic units of this siliciclastic-dominated mixed system are markedly different to the ones observed in present and ancient carbonate-dominated mixed systems, but they show strong similarities with the products of storm-dominated, pure siliciclastic shoreface–shelf systems. Basin-scale depositional controls, such as arid climatic conditions and shallow epeiric seas might aid in the development of mixed systems across the full spectrum (i.e. from carbonate-dominated to siliciclastic-dominated end members), but the interplay of processes supplying sand to the system, as well as processes transporting sediment across the marine environment, are key controls in shaping the tridimensional facies distribution and the genetic units of siliciclastic-dominated mixed systems. Thus, the identification of different combinations of basin-scale factors and depositional processes is key for a better prediction of conventional and unconventional reservoirs within mixed, carbonate–siliciclastic successions worldwide.

Keywords Depositional controls, Lower Cretaceous, mixed carbonate–siliciclastic marine systems, Neuquén Basin, Pilmatué Member, sequence stratigraphy.

INTRODUCTION

Mixed carbonate–siliciclastic systems are defined as those depositional settings where coeval deposition of carbonate and siliciclastic sediment takes place (Mount, 1984; Goldhammer, 2003), which is in contrast to mixed carbonate–siliciclastic successions in which reciprocal sedimentation (Van Siclen, 1964) results in the formation of high-frequency alternation of pure carbonate and siliciclastic units that represent different depositional systems (Schwarz *et al.*, 2016b). Depositional models for shallow-marine, mixed carbonate–siliciclastic systems, the focus of this study, are far from being understood.

The configuration and evolution of these mixed systems depend heavily on the processes responsible for producing different types of carbonate grains (i.e. skeletal and non-skeletal), as well as the processes supplying siliciclastic sand and mud to a basin (Zonneveld *et al.*, 2001; Coffey & Sunde, 2014; D'Agostini *et al.*, 2015; Zeller *et al.*, 2015; Labaj & Pratt, 2016). Hydrodynamic processes transporting and depositing the sediment within the marine realm control the final mixing. Although facies distribution schemes have been proposed for some modern mixed shelves and ramps in which carbonate sediment prevails (Purdy & Gischler, 2003; Gischler & Lomando, 2005), less studies have reported on modern or Cainozoic, mixed shallow-marine systems in which siliciclastic sediment is dominant, which is commonly mixed with skeletal grains (Saul *et al.*, 1999; Cantalamessa *et al.*, 2005; Vital *et al.*, 2008). However, even more uncommon are reconstructions of siliciclastic-dominated systems from the rock record in which the contribution of non-skeletal grains is important (Coffey & Sunde, 2014). As a result, no previous studies have attempted to show the degree of variability that can exist from carbonate-dominated to siliciclastic-dominated systems, and their resulting stratigraphic patterns, within the spectrum of these mixed systems.

The Pilmatué Member of the Agrio Formation in the study area (central Neuquén Basin) is a mixed carbonate–siliciclastic unit (Schwarz *et al.*, 2016a), in which both lateral and vertical transitions from pure siliciclastic, to mixed, to pure carbonate rocks are recorded, but with a pre-eminence of siliciclastic sediment. It thus provides an opportunity to reconstruct in detail the depositional systems, their short-term evolution and the resulting stratigraphic (genetic) units produced in mixed systems with a dominance of siliciclastic supply. The aims of this article are therefore to: (i) reconstruct depositional systems and sequence architecture by describing and interpreting facies associations of the unit over a 350 m thick succession and 20 km long transect; (ii) recreate the short-term shoreline evolution and longer term palaeogeographic scenarios; and (iii) discuss controls on the formation of mixed carbonate–siliciclastic systems and their potential variability even within a single basin.

GEOLOGICAL SETTING

The Neuquén Basin is located in west-central Argentina, covering most of the Neuquén Province, and significant parts of Mendoza, La Pampa and Río Negro provinces (Fig. 1A). It is bounded by tectonically stable regions to the north-east (Sierra Pintada System) and south-east (North Patagonian Massif), and its sedimentary record accumulated in a variety of basin styles during the Late Triassic to the early Cenozoic (Legarreta & Uliana, 1991; Howell *et al.*, 2005). The basin, which is one of the most important petroleum provinces of South America, can be divided into two regions: the Andean Thrust and Fold belt with extensive outcrops of Jurassic–Cretaceous strata, and the Neuquén Embayment, with slightly deformed strata in the subsurface.

Between the Tithonian and Hauterivian ages, the Neuquén Basin was a back-arc basin (Fig. 1B) characterized by a ramp-type gradient in the eastern and southern margins (Legarreta & Uliana, 1991; Spalletti *et al.*, 2000), but a more inclined depositional profile towards the emergent magmatic arc (Spalletti *et al.*, 2008). During that interval, long-lived periods of highstand conditions were interrupted by significant events of relative sea-level fall that, in turn, were followed by rapid transgressions (Fig. 2A). Relative sea-level drops triggered partial disconnection of the epeiric sea from the proto-Pacific, as well as the exposure and erosion of large areas of the basin (Howell *et al.*, 2005). Two of these transgressive–regressive cycles were first recognized by Weaver (1931) and Groeber (1946) and comprise parts of the Agrio Formation. The Pilmatué Member, the focus of this study, represents the older one (Fig. 2A).

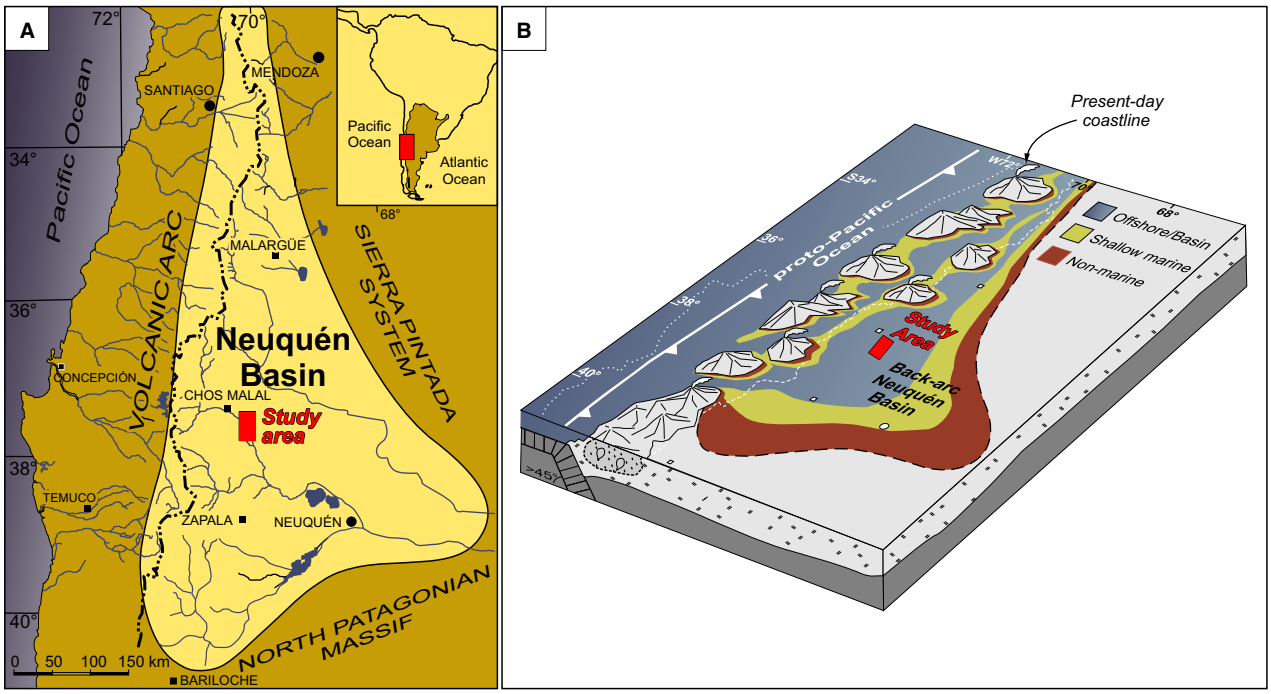

Fig. 1. (A) Location map of the Neuquén Basin. (B) Schematic geological setting of the Neuquén Basin during the Early Cretaceous (after Howell *et al.*, 2005; Schwarz *et al.*, 2006). During this period, the basin constituted an epeiric sea, partially connected to the proto-Pacific Ocean trough gaps in the volcanic arc. The study area (Fig. 3) is shown in both panels.

PILMATUÉ MEMBER STRATIGRAPHY

The Pilmatué Member of the Agrio Formation is a regionally extensive unit dominated by marine deposits, which accumulated across the Neuquén Basin between the late Valanginian and early Hauterivian (Spalletti *et al.*, 2011). It is a mixed carbonate–siliciclastic unit (Weaver, 1931; Groeber, 1946), and its base marks a deepening with respect to the underlying continental or shallow-marine deposits of the Mulichinco Formation (Schwarz & Howell, 2005). At the top, the Pilmatué Member is abruptly truncated by continental (fluvial and aeolian) deposits of the Avilé Member of the Agrio Formation (Fig. 2A), which represents a second-order lowstand stage (Legarreta & Uliana, 1991; Veiga *et al.*, 2002, 2007).

The Pilmatué Member was included in studies addressing basin-wide palaeogeographic reconstructions (Legarreta & Gulisano, 1989; Legarreta & Uliana, 1991, 1999) and in detailed palaeontological studies (Aguirre-Urreta *et al.*, 2005; Lazo, 2006), but the palaeoenvironmental and sequence-stratigraphic evolution of the unit has only been broadly outlined (Lazo, 2007; Spalletti *et al.*, 2011). Detailed reconstructions of depositional systems have become available recently for southern regions of the basin (Schwarz *et al.*, 2016c; Veiga & Schwarz, 2017), but not for the study area in its central sector (Fig. 1).

In this region of the Neuquén Basin, the Pilmatué Member comprises up to 700 m of marine deposits and is dominated by basinal shale and offshore mudstone, with subordinate shallow-marine siliciclastic sandstone and mixed (carbonate–siliciclastic) sandstone (Schwarz *et al.*, 2016a). Time-equivalent marginal-marine and continental deposits are more abundant to the east in the Neuquén Embayment (Lower Centenario Member; Digregorio & Uliana, 1980), but this transition is poorly understood. In the northern sector of the basin (Mendoza Province), the Pilmatué Member is mostly composed of basinal and offshore carbonate mudstone and marl (Sagasti, 2005).

An ammonite biostratigraphic framework has been erected for the Pilmatué Member (Aguirre-Urreta *et al.*, 2005, 2011), indicating that the unit spans from the late Valanginian to the early Hauterivian (Fig. 2B). Four ammonite zones are identified in this unit: *Pseudofavrella*

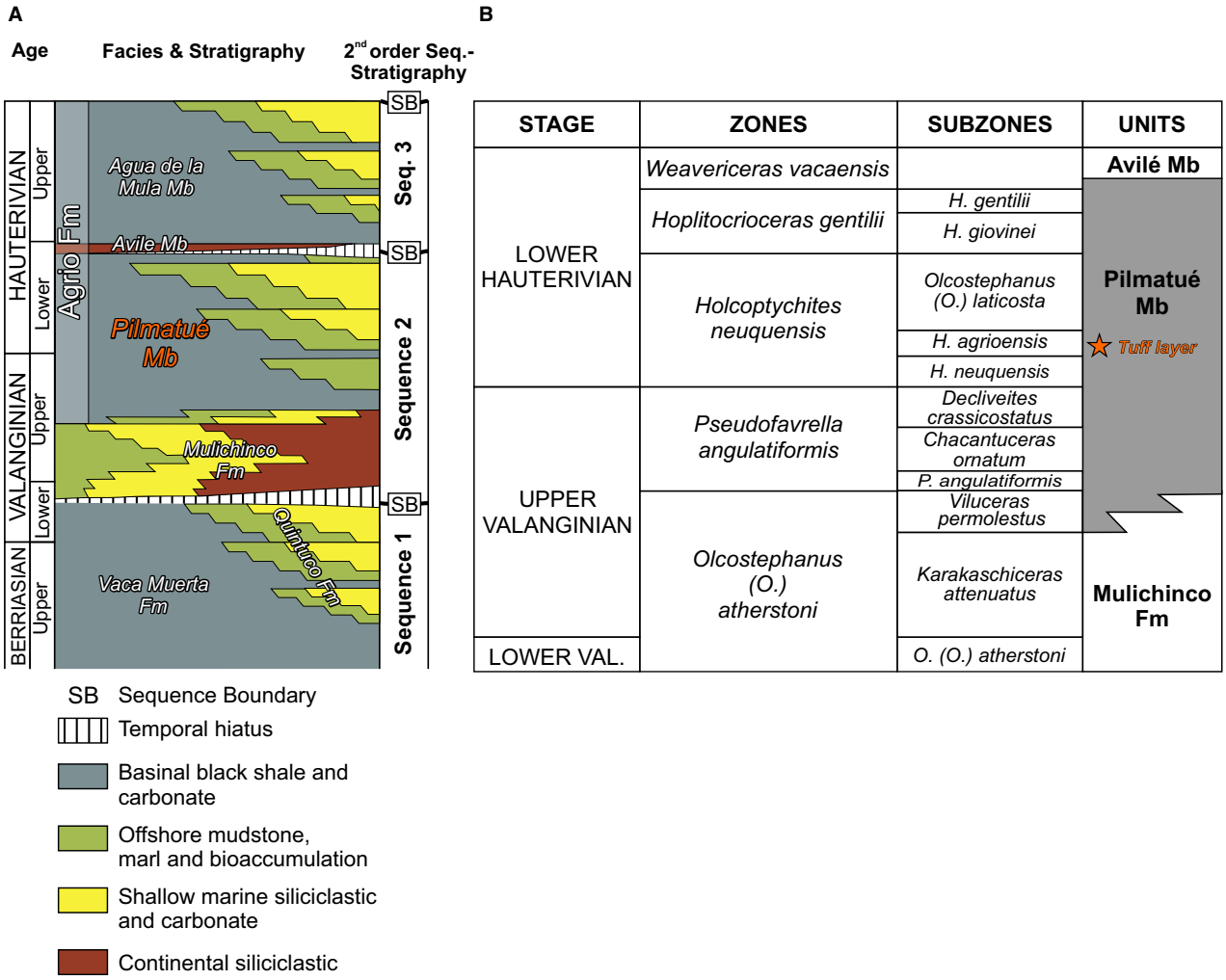

Fig. 2. (A) Chronostratigraphic chart for the late Tithonian – late Hauterivian of the Neuquén Basin (modified from Schwarz *et al.*, 2006). The base of the Pilmatué Member of the Agrio Formation represents a major flooding of the basin. (B) Valanginian–early Hauterivian biostratigraphic scheme for the Pilmatué Member of the Agrio Formation (compiled from Aguirre-Urreta *et al.*, 2005, 2011), showing the time-transgressive basal boundary in the eastern sector of the basin, where it overlies shallow-marine and continental deposits of the Mulichinco Formation. The stratigraphic location of the tuff layer dated by Schwarz *et al.* (2016a) is also shown.

angulatiformis, *Holcoptychites neuquensis*, *Hoplitocrioceras gentilii* and *Weaviceras vacaensis* (Fig. 2B), which are recognized across the basin (Aguirre-Urreta *et al.*, 2005, 2011).

STUDY AREA AND METHODS

The study area is located in the central sector of the Neuquén Basin, near the town of Chos Malal, between 37°42′S and 37°28′S, and 69°59′W and

Fig. 3. Simplified geological map of the studied area; the Pilmatué Member is exposed in three north–south oriented anticlines. The 20 sedimentological sections of the unit analysed in this contribution are shown. PL: Puesto Ladrillo, S15: South 15, PM: Puesto Mardone, LR: Loma Rayoso, CD: Cóndores, AN: Anfiteatro, PR: Puesto Riquelme, EC: El Cierre, SZ: Solorza, RN: Río Neuquén, QG: Quebrada Grande, QC: Quebrada Chica, PA: Puesto Abandonado, EA: El Abra, SE: San Eduardo, PLe: Puesto Leiva, CC: Cerro Curaco, PH: Puesto Habitado, ECu: Escuela Curaco, PG: Puesto González. The inset (right side) shows the projection of all the sections in a south–north-oriented transect, which is used to reconstruct the general stratigraphy of the unit (shown in Fig. 4).

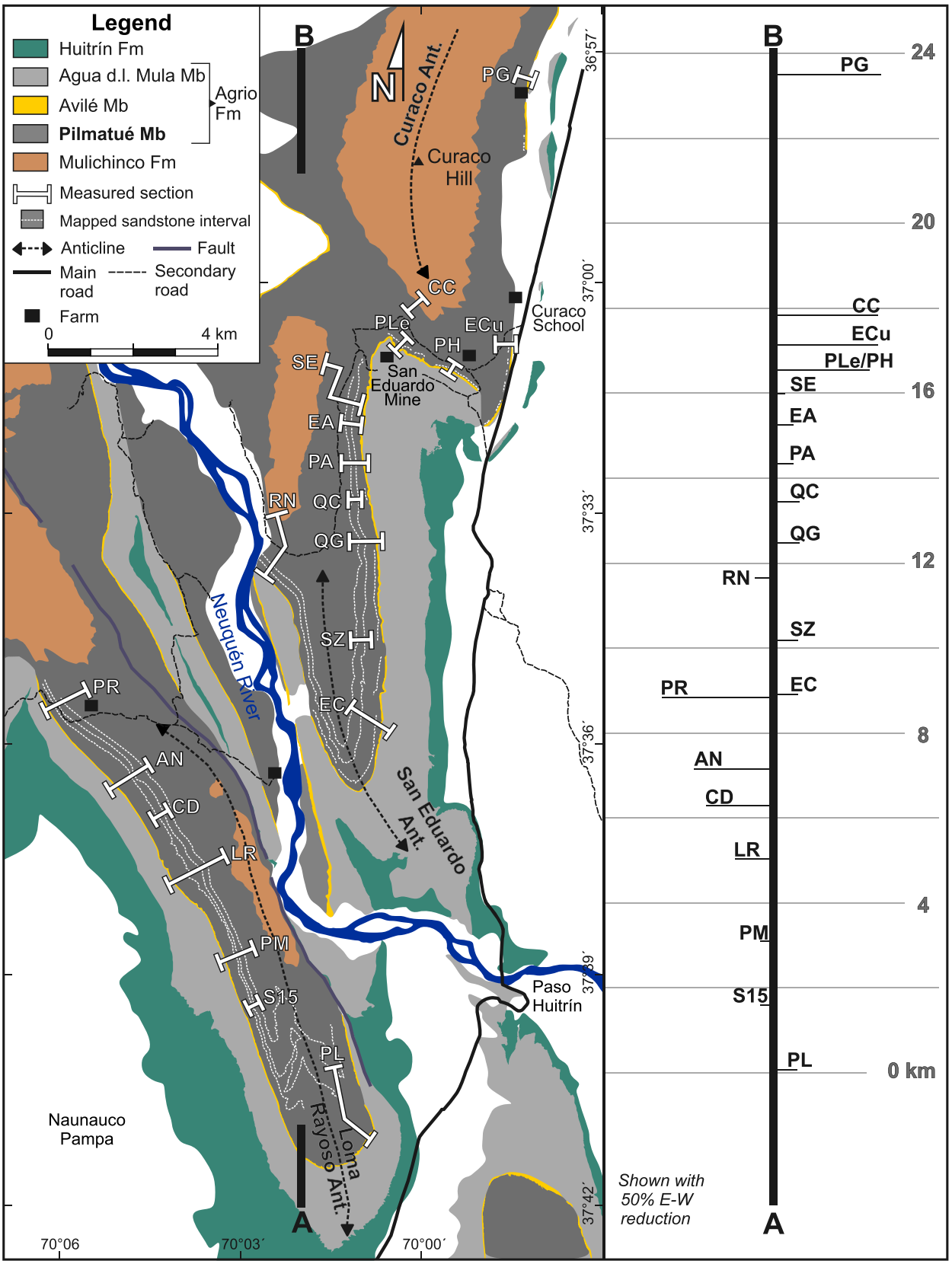

70°05′W (Figs 1 and 3). This region represents the eastern limit of the Agrio Fold and Thrust Belt, and the Pilmatué Member crops out along three anticlines that collectively represent a continuous, accessible and poorly vegetated outcrop, which is *ca* 25 km long and up to 8 km wide (Fig. 3). Only in the northernmost 4 km of the area is the stratigraphic section not fully exposed (Fig. 4).

In the study area, the lower half of the Pilmatué Member is exclusively composed of fine-grained lithologies, including grey shale and marl, greenish mudstone and sandy mudstone. The upper half of the unit is characterized by fine-grained deposits interbedded with coarsening-upward, decametre thick intervals comprising muddy sandstone, fine-grained sandstone, mixed sandstone–carbonate deposits and skeletal carbonate (Fig. 4). This section, up to 350 m thick, is the focus of this study. Northward of the study area (central and northern part of Curaco anticline), sandstone packages are almost absent, suggesting a general proximal–distal trend in that direction (Fig. 4). Biostratigraphically, the study interval comprises the lower Hauterivian ammonite zones, from the *Holcoptychites neuquensis* Zone at the base, to the *Weavericeras vacaense* Zone in its upper contact with the Avilé Member (Fig. 4). The Hauterivian age at the base of the study interval was recently confirmed by a U-Pb dating of 130·0 ± 0·8 Ma (Schwarz *et al.*, 2016a).

The studied succession was investigated by logging 20 key sections, typically less than 2 km apart (Figs 3 and 4). Shorter supplementary sections were measured to capture rapid lateral facies transitions. Sedimentological data were recorded in each section (texture, sedimentary structures and palaeocurrents). Ichnofaunal, macrofaunal and taphonomic information was also collected. Bioturbation intensity was characterized using the Bioturbation Index (BI) defined by Taylor & Goldring (1993). Key stratigraphic surfaces (mostly transgressive surfaces; Fig. 4) were walked out and mapped laterally in the field. Measured sections and outcrop mapping were combined with correlations based on high-resolution aerial photographs of the outcrops (Fig. 5). The photographs provided a continuous view of the succession along the main exposures. Interpretation of macrofossil associations followed previous palaeoecological studies on the Pilmatué Member in the

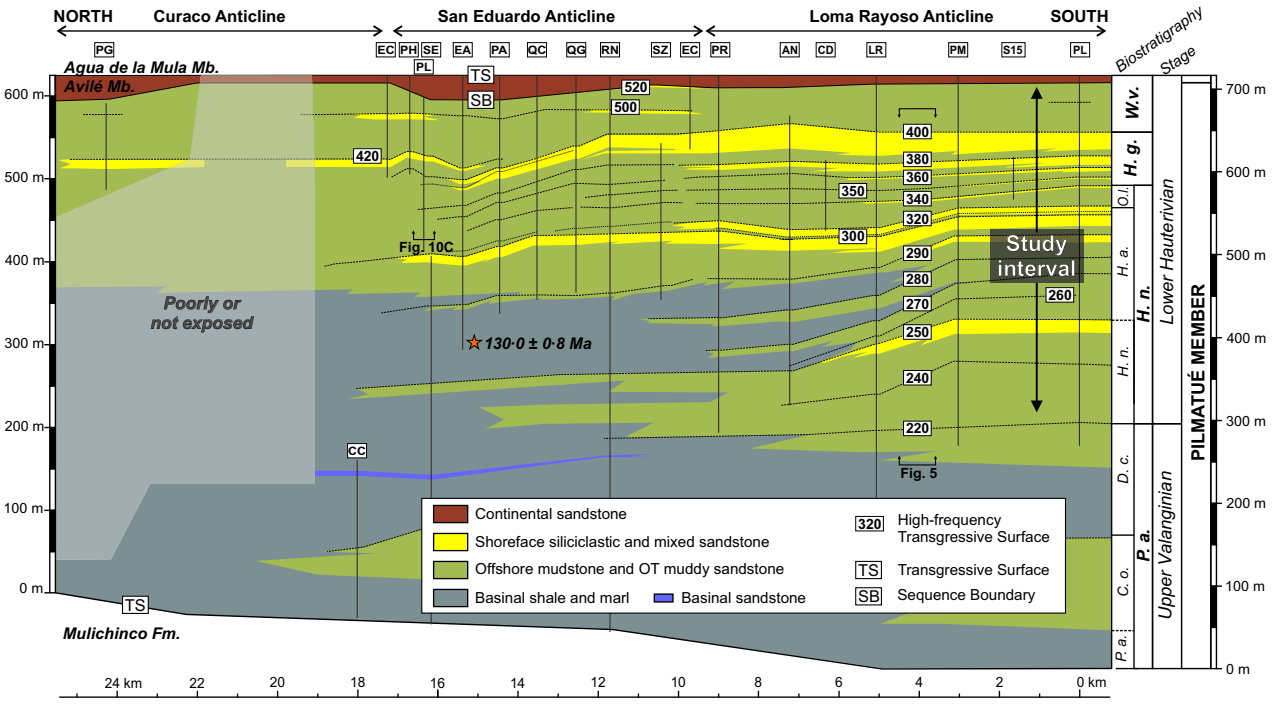

Fig. 4. Summary stratigraphic cross-section of the Pilmatué Member in the Loma Rayoso-San Eduardo region. Biostratigraphic subdivisions after Schwarz *et al.* (2016a). The datum horizon is the regionally extensive transgressive surface marking the base of the Agua de la Mula Member of the Agrio Formation. Shoreface-offshore tongues are here defined as parasequences and numbered using arbitrary number from PS220 to PS520. The transgressive surfaces bounding these parasequences at their bases are labelled consequently (for example, PS220 is bounded by transgressive surface TS220).

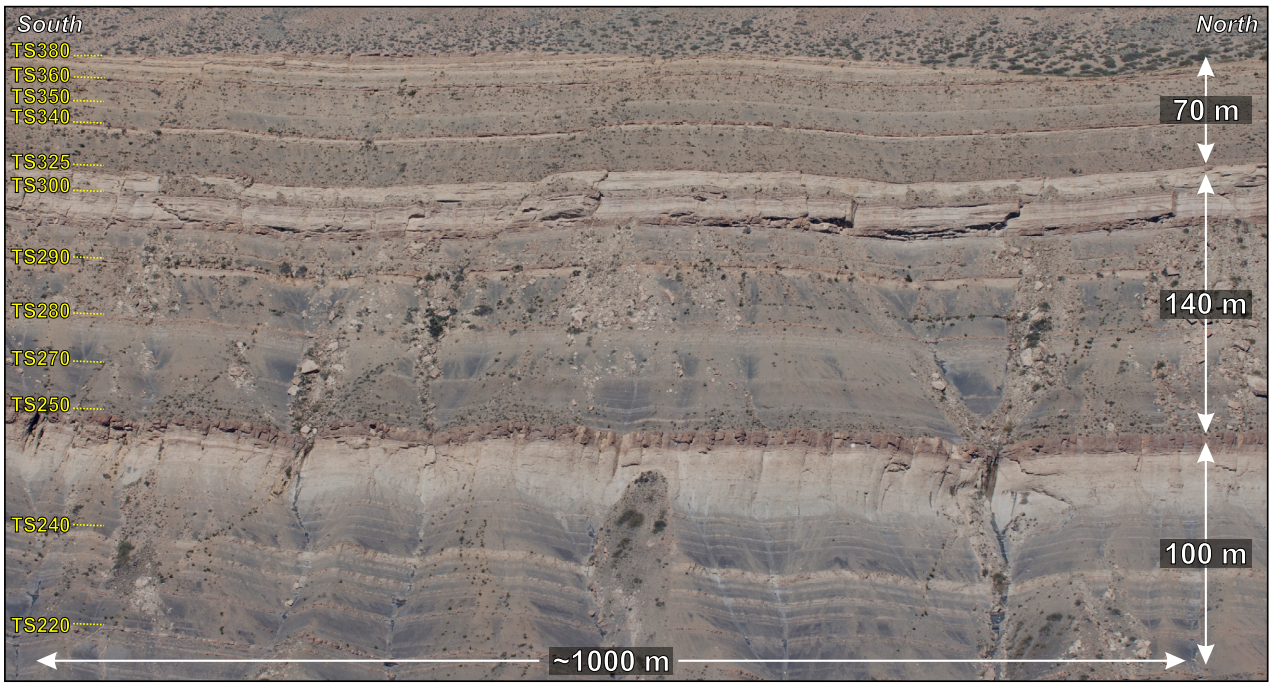

Fig. 5. Low-angle, high-resolution aerial photograph between Puesto Mardone and Loma Rayoso sections showing most of the study interval (looking west). Transgressive surfaces (TS220 to TS380) mark the bounding surfaces between successive parasequences (for example, PS240 is bounded by TS220 and TS240). Parasequences PS400 to PS520 are topographically below PS380 and not seen in the picture.

southern sector of the basin (Lazo, 2007). Petrographical analysis of 70 thin sections helped to characterize the sedimentary texture and composition of individual beds. Percentages of siliciclastic and carbonate components, as well as grain-size distributions, were estimated using visual comparative charts (cf. Scholle & Ulmer-Scholle, 2003).

FACIES ASSOCIATIONS

Seven facies associations were identified and interpreted in the early Hauterivian succession of the Pilmatué Member. Three siliciclastic and two mixed facies associations show systematic vertical transitions and are interpreted to represent different conditions across a shelf to shoreface depositional system: basin (i.e. distal shelfal setting without adjacent slope; BA); offshore (OF); offshore-transition (OT); lower shoreface (LS); and upper shoreface (US) facies associations (Fig. 6; Table 1). Two additional facies associations are dominantly composed of gravel-size skeletal fragments and are here collectively termed as shell beds (Table 1): shoreface shell beds (SSB) and offshore shell beds (OSB).

Basin (BA)

Description

This facies association is composed of fissile, dark grey to black shale (Fig. 7A). Although fissility is ubiquitous (BI 0 to 1), a structureless appearance is observed locally. Apart from ammonites, macrofossils are not present in the shale, but microfossils such as foraminifera and radiolarians are frequent (Table 1).

Interpretation

This association is interpreted as the product of settling from suspension on a low-energy, poorly oxygenated sea floor, most likely in a siliciclastic–carbonate basinal setting located well below storm-wave base (Spalletti *et al.*, 2001).

Offshore (OF)

Description

This facies association comprises coarsening-upward intervals with massive, siliciclastic mudstone at the base that grade upward to structureless siltstone (Fig. 7B). Macrofossils are uncommon, but articulated specimens of shallow-burrowing bivalves such as *Cucullaea* sp.

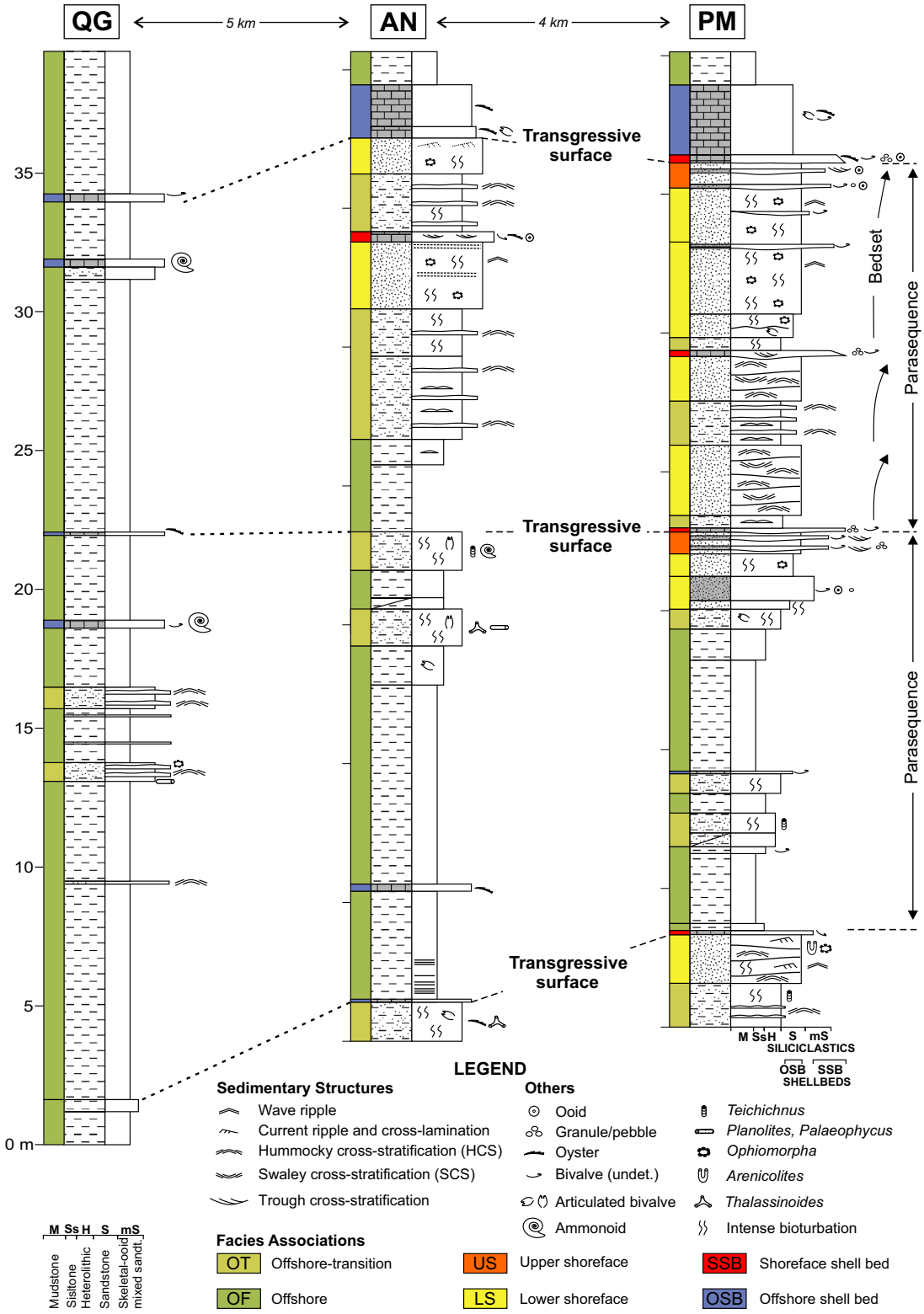

Fig. 6. Selected sedimentological sections from the Pilmatué Member in the Loma Rayoso-Sand Eduardo region, showing key facies, facies associations (except basinal association), stacking patterns and bounding surfaces. Interpreted genetic units (i.e. parasequences and bedsets) are indicated in one case as an example. *Bivalve (undetermined)* refers to all the bioclasts that come from endobenthic and semi-endobenthic organisms that are not oysters.

Table 1. Description and interpretation of facies associations recognized in the Pilmatué Member. A: articulation degree; F: fragmentation degree; D: distribution; BI: bioturbation index (1 to 6); l: low; m: moderate; h: high. Epibenthic macrofossils: *Ceratostreon* sp. (oyster), *Parsimonia* sp. (serpulid), *Columastrea* sp. (coral). Endobenthic macrofossils: *Eriphyla* sp., *Cucullaea* sp. and *Steimanella* sp. are shallow-burrowing bivalves; *Panopea* sp., *Ptychomya* sp. and *Pholadomya* sp. are deep-burrowing bivalves. Semi-endobenthic macrofossils: *Pinna* sp. and pectinids are byssate bivalves, and *Aetostreon* sp. is a reclined oyster.

Facies association	Lithology	Sedimentary structures; thickness	Trace fossils; fossils	Taphonomy	Interpretation. Depositional setting
Basin (BA)	Dark grey to black siliciclastic and carbonate shale	Fissility, uncommon structureless; <95 m thick	Typically barren (BI 0 to 1); ammonites, foraminifera, radiolarians	A: h, F: l	Settling from suspension on a low-energy, poorly oxygenated sea floor. Mixed siliciclastic–carbonate basinal setting
Offshore (OF)	Light grey to greenish siliciclastic mudstone and siltstone	Massive, subordinate lamination; <35 m thick	*Thalassinoides*, *Chondrites* (BI 5 to 6); *Cucullaea* sp., *Eriphyla* sp., *Steimanella* sp.	A: h-m, F: l, D: *in situ* or parallel to bedding	Settling from suspension on a low-energy, well-oxygenated sea floor. Siliciclastic offshore
Offshore-transition (OT)	Mudstone and siltstone interbedded with very fine-grained sandstone, rare rip-up muddy clasts	Dominant lenticular and wavy bedding with cross-lamination and symmetrical ripples (beds <0·05 m thick), subordinate hummocky cross-stratification (sets <0·20 m), rare gutter casts and parting lineation; <9 m thick	Resident (BI 3 to 6); *Palaeophycus*, *Thalassinoides, Teichichnus*, *Planolites, Asterosoma, Rosselia, Ophiomorpha*, opportunistic (BI 1 to 3); *Ophiomorpha, Gyrochortes*; *Panopea* sp., *Eriphyla* sp., *Steimanella* sp., *Pinna* sp.	A: h-m, D: pockets and stringers of *Pinnas,* frequently in life position	Alternation of settling from suspension and sandy distal storm events, below fair-weather wave base and above storm base, *Cruziana* ichnofacies suite. Transition zone from offshore to shoreface
Lower shoreface (LS)	Very fine and fine-grained sandstone, rare rip-up clasts and gravel and sand-size shells	Dominant isotropic and anisotropic hummocky cross-stratification, subordinate swaley cross-stratification, current-ripple cross-lamination, small symmetrical 3D ripples, rare parting lineation and gutter casts; <9 m thick	*Ophiomorpha*, *Skolithos*, *Palaeophycus, Arenicolites*, *Gyrochortes, Rosselia* (BI 1 to 6); Rare *Steimanella* sp.	–	Large asymmetrical ripples and hummocks by oscillatory and combined storm-related flows, Wave-induced fair-weather conditions, *Skolithos* ichnofacies suite. Storm-dominated, wave-influenced lower shoreface

Table 1. (continued)

Facies association	Lithology	Sedimentary structures; thickness	Trace fossils; fossils	Taphonomy	Interpretation. Depositional setting
Upper shoreface (US)	Fine to medium-grained siliciclastic sandstone, rare coarse-grained to pebble-size clasts, common ooids, common to rare gravel to sand-size bioclasts	Trough and planar cross-bedding (sets <0·30 m thick and <2·0 m wide or 0·50 to 1·0 m thick and 2 to 5 m wide), subordinate current-ripple tops; <5 m thick	*Ophiomorpha*, *Arenicolites* (BI 0 to 2); Undetermined bivalves, oysters	–	Dune migration under unidirectional currents, resident *Skolithos* ichnofacies suite. Upper shoreface conditions
Shoreface shell beds (SSB)	Ooid-skeletal grainstone-rudstone, abundant sand-size and gravel-size (<150 mm) bioclasts and siliciclastic fine sand, common ooids, common to rare siliciclastic coarse sand to pebbles, rare early-cemented rip-up sandstone clasts, grading to skeletal-ooid packstone	Cross-bedding (sets <0·10 m thick and <0·60 wide) in well-sorted facies, or massive in poorly sorted facies, rare large symmetrical ripples with straight to slightly sinuous and rounded crests; commonly <0·50 m thick, rarely up to 2·0 m thick	Locally abundant *Thalassinoides*; *Ceratostreon* sp., *Pholadomya* sp., *Ptychomya* sp., *Steimanella* sp., *Trigonia* sp., echinoids, gastropods	–	Allochthonous to parautochthonous macrofossil assemblages, intense, infrequent physical reworking near or below fair-weather wave base by wave action and storm-related flows. Shoreface and offshore-transition, during transgressive conditions
Offshore shell beds (OSB)	Skeletal, lime mud-rich floatstone, dominant gravel-size bioclasts, less sand-size bioclasts, terrigenous silt, glauconite and ooids	Massive; commonly <0·5 m thick, rarely up to 1·5 m thick	Uncommon *Thalassinoides; Ceratostreon* sp., *Parsimonia* sp., *Columastrea* sp., *Eriphyla* sp., *Cucullaea* sp., *Panopea* sp., *Ptychomya* sp., *Pholadomya* sp., *Steimanella* sp., *Aetostreon* sp., pectinids, ammonites	A: h-m, F: m-l, D: chaotic, some in life position	Parautochthonous to autochthonous macrofossil assemblages, low net accumulation rates, minimum physical reworking. Offshore, during transgressive conditions

and *Steimanella* sp. are present locally (Table 1). Bioturbation intensity is high (BI 5 to 6) but, apart from a few *Thalassinoides* and *Chondrites*, individual traces are hard to identify.

Interpretation

This association is interpreted to reflect mostly settling from suspension on a well-oxygenated, low-energy sea floor, below the storm-wave base (Spalletti *et al.*, 2011). Compared to the previous association, in this distal setting siliciclastic supply was high enough to significantly dilute any carbonate contribution derived from pelagic rain. Silt-dominated intervals could have also originated by across shelf flows (Hill *et al.*, 2007; Parson *et al.*, 2007), but the final structureless character precludes further interpretation.

Offshore-transition (OT)

Description

This facies association is composed of heterolithic deposits, muddy sandstone and subordinate hummocky cross-stratified sandstone (Fig. 6; Table 1). Heterolithic deposits are mostly composed of siltstone interbedded with lenticular sandstone that has cross-lamination and symmetrical rippled tops (Fig. 7C); they range from mud-dominated to sand-rich heterolithic intervals with moderate bioturbation (BI 3 to 4), typically forming metre-scale coarsening-upward successions. In contrast, the muddy sandstone is heavily bioturbated (BI 5 to 6), with up to 35% disseminated mud (Fig. 7D).

The trace fossil assemblage in these facies includes *Asterosoma*, *Ophiomorpha*, *Palaeophycus*, *Planolites*, *Rosselia*, *Teichichnus* and *Thalassinoides*. Macrofossils are not common, but when present, they are mostly represented by moulds of deep-burrowing and shallow-burrowing bivalves, mostly articulated and locally in life position (Fig. 7D). Sandstone beds with hummocky cross-stratification (HCS) are interbedded both within heterolithic strata and bioturbated muddy sandstone (Fig. 7E). The beds show parting lineation, and both symmetrical and asymmetrical small ripples (*sensu* Dumas *et al.*, 2005) can occur on top of the beds. *Ophiomorpha* and *Gyrochortes* are common in these HCS beds, which have low to moderate bioturbation index (BI 1 to 3). Ripple crests both in heterolithic deposits and HCS beds (Fig. 7E) are oriented mostly east–west with preferential northward migration in asymmetrical forms.

Interpretation

The large proportion of mudstone layers, as well as the mud fraction within muddy sandstone beds, suggest that bottom energy conditions were frequently low enough to allow mud deposition and preservation in this setting (Morris *et al.*, 2006; Schwarz *et al.*, 2016b). Sandy beds are related to storm-generated flows, and both symmetrical and asymmetrical small ripples probably formed under purely oscillatory or combined flows (Myrow & Southard, 1996; Dumas *et al.*, 2005). Most of the silt and very fine sand, however, was subsequently mixed with mud due to intense bioturbation. This is supported by the diverse deposit feeding dominated trace fossil assemblage, interpreted to represent a *Cruziana* ichnofacies (MacEachern *et al.*, 2007a). Storm-surge flows carrying larger volumes of sand created hummocky bedforms under combined, high-velocity flows (Myrow & Southard, 1996; Dumas *et al.*, 2005) and their final deposits escaped complete homogenization.

This facies association is interpreted to represent a storm-dominated offshore–shoreface transition, between storm-wave base and fair-weather wave base (Reading & Collinson, 1996), with storm-generated flows preferentially oriented from south to north (i.e. shore-normal to the shoreline). Metre-scale coarsening-upward intervals may record shallowing-upward events (Walker & Plint, 1992) or a gradual increase in storm regime (Hampson & Storms, 2003).

Lower shoreface (LS)

Description

This facies association grades vertically from the OT facies association and comprises the amalgamation of sandstone beds having variable physical sedimentary structures, as well as intensely bioturbated sandy packages (Fig. 6; Table 1). Beds of very fine-grained sandstone with HCS are dominant (Fig. 7F), in some cases associated with horizontal lamination, low-angle lamination or swaley cross-stratification. Sandstone beds with ripple cross-lamination are less abundant, and they typically have tops with slightly asymmetrical or symmetrical ripples. Cross-lamination orientation is variable, but southward migration dominates. Bioturbation index is low to moderate (BI 1 to 4) in these cross-stratified facies. Burrowing intensity varies from high to very high (BI 4 to 6) in the bioturbated sandstone facies, and HCS or ripple cross-lamination is faintly preserved. *Ophiomorpha* is dominant in

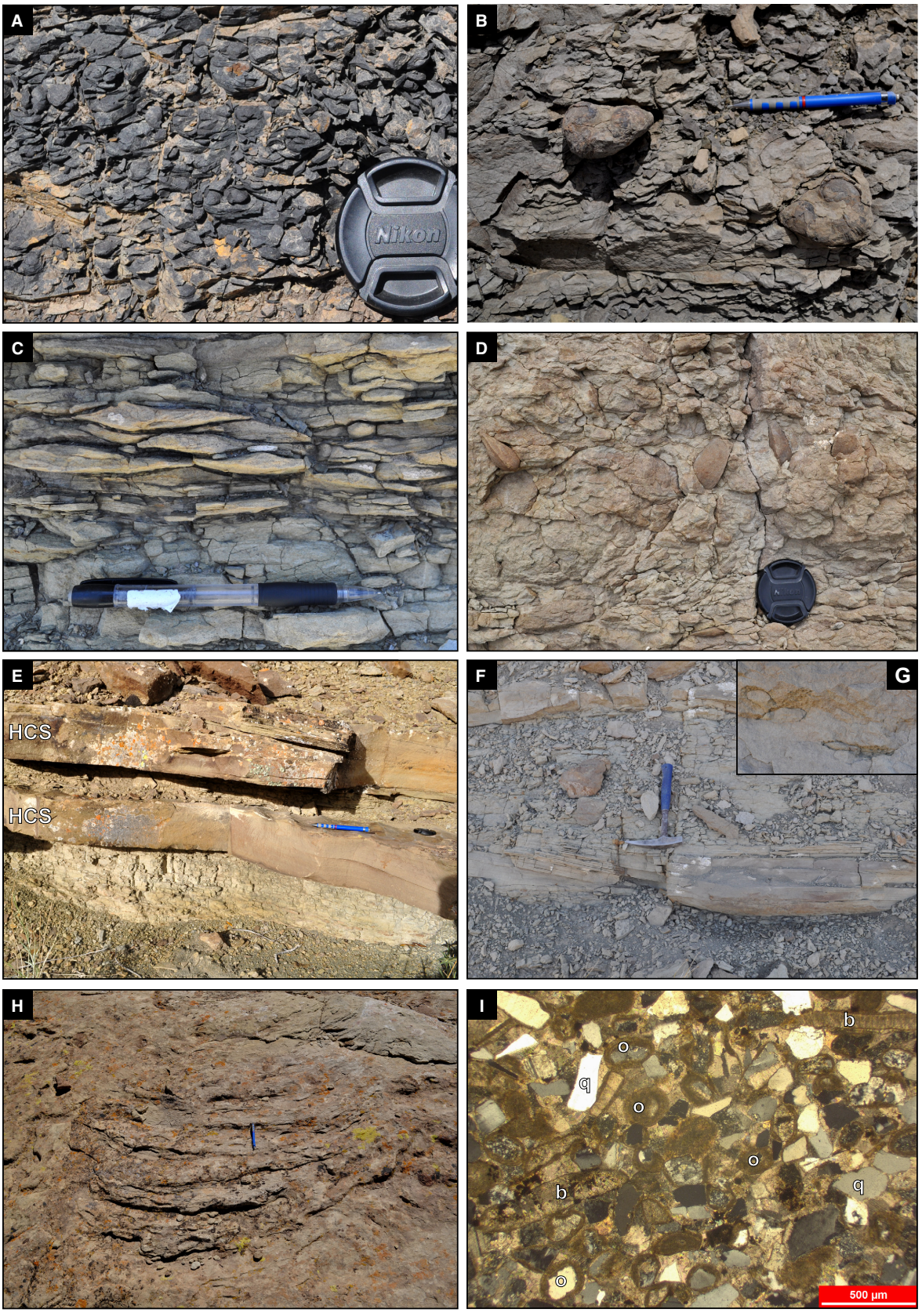

Fig. 7. Main attributes of siliciclastic and mixed (carbonate–siliciclastic) facies associations. (A) Fissile, dark grey shale of the BA facies association. (B) Massive, light grey mudstone with *in situ*, articulated macrofossils (*Cucullaea* sp.) belonging to the OF association. (C) Sandstone-dominated heterolithic deposits with symmetrical ripples. (D) Bioturbated, muddy sandstone of the OT facies association. In (D), note the internal moulds of *Panopea* sp. resting approximately in life position. (E) Discrete sandstone beds interbedded within heterolithic deposits in the OT association, showing hummocky cross-stratification and rippled tops (indicated by pencil). (F) Amalgamated sandstone beds having HCS and ripple cross-lamination, typical of the LS facies association. (G) Bioturbated, very fine-grained and fine-grained sandstone that also characterize this association. *Ophiomorpha* burrows are dominant. (H) Plan view of siliciclastic, fine-grained sandstone with trough cross-stratification typical of the US association. (I) Thin section photograph (cross-polarized light) of well-sorted, mixed sandstone comprising ooids, bioclasts and siliciclastic sand-size grains, which also belong to the US facies association. Legend: b – bivalve; o – ooid; q – quartz. Lens cap is 4·5 cm in diameter, pencils are *ca* 14 cm in length, and hammer is 33 cm long.

the bioturbated facies (Fig. 7G), together with subordinate *Arenicolites*, *Gyrochortes*, *Palaeophycus*, *Rosselia* and *Skolithos*, which can also be present in all of the facies. Isolated shells of endobenthic bivalves (*Steimanella* sp.) are uncommon.

Interpretation

The amalgamated sandstone packages are interpreted to reflect a lower shoreface setting, where sand was mostly transported and deposited by storm-related flows and fair-weather waves, but mud, if ever deposited, was not preserved (Walker & Plint, 1992). The HCS-dominated packages are related to storm-generated, offshore-oriented currents that most commonly created and preserved hummocky bedforms under combined flows. However, plane bed conditions under combined flows were also generated, probably suggesting relatively more energetic flows (Arnott, 1993; Perillo *et al.*, 2014). Protected areas or time intervals with less storm activity favoured aggradation of onshore migrating ripples under fair-weather conditions. This situation was commonly associated with intense biogenic reworking by a filter-feeder dominant *Skolithos* ichnofacies assemblage (MacEachern *et al.*, 2007a).

Upper shoreface (US)

Description

This facies association is mostly composed of fine-grained, cross-stratified, siliciclastic sandstone and mixed carbonate–siliciclastic sandstone (Fig. 6; Table 1). In the siliciclastic sandstone, cross-sets range from small scale (<0·30 m thick and <2·0 m wide; Fig. 7H) to larger sets up to 1 m thick and 5 m wide. Mixed sandstone commonly occurs as subordinate lenses within the siliciclastic sandstone, typically in the lower part of the troughs of cross-bed sets; they are characterized by the unusual concentration of gravel-size bioclasts, in some cases together with siliciclastic coarse material (coarse sand to fine pebble). However, mixed sandstone also exists as discrete intervals up to 2 m thick of better sorted sand-size material that is mostly ooids, bioclasts and terrigenous grains (Fig. 7I). In this mixed facies, trough cross-sets are typically of small scale (<0·20 m thick and <1·5 m wide). Bioturbation is usually absent to low (BI 0 to 2) in all the facies of this association, and is represented by sparse *Ophiomorpha* and *Skolithos*. Palaeocurrent direction from trough axes shows a wide variation, but northward to eastward directions predominate (mean to the north-east). Current ripples are commonly associated with cross-bedded sets, but they show a wide range of crest orientations.

Interpretation

This facies association reflects the development of relative permanent unidirectional currents that formed subaqueous dunes in an upper shoreface setting (Walker & Plint, 1992; Clifton, 2006). These bedforms were probably produced in bar troughs and/or rip channels, and preferential concentration of gravel-size bioclasts and terrigenous sand and pebbles was present at the base of these depressions. Low bioturbation suggests unstable, mobile substrates uncommonly colonized by a proximal *Skolithos* ichnofacies suite. Abundant sand-size bioclasts and ooids in this upper shoreface facies suggest fairly continuous mixing of *in situ* produced carbonates together with siliciclastic grains.

Shoreface shell beds (SSB)

Description

These shell beds are thin with erosional bases, and they comprise two distinct facies (Table 1). One facies type is characterized by small-scale cross-bedded, oolitic–skeletal grainstone (Fig. 8A and B). Fragmented, gravel-size bioclasts are

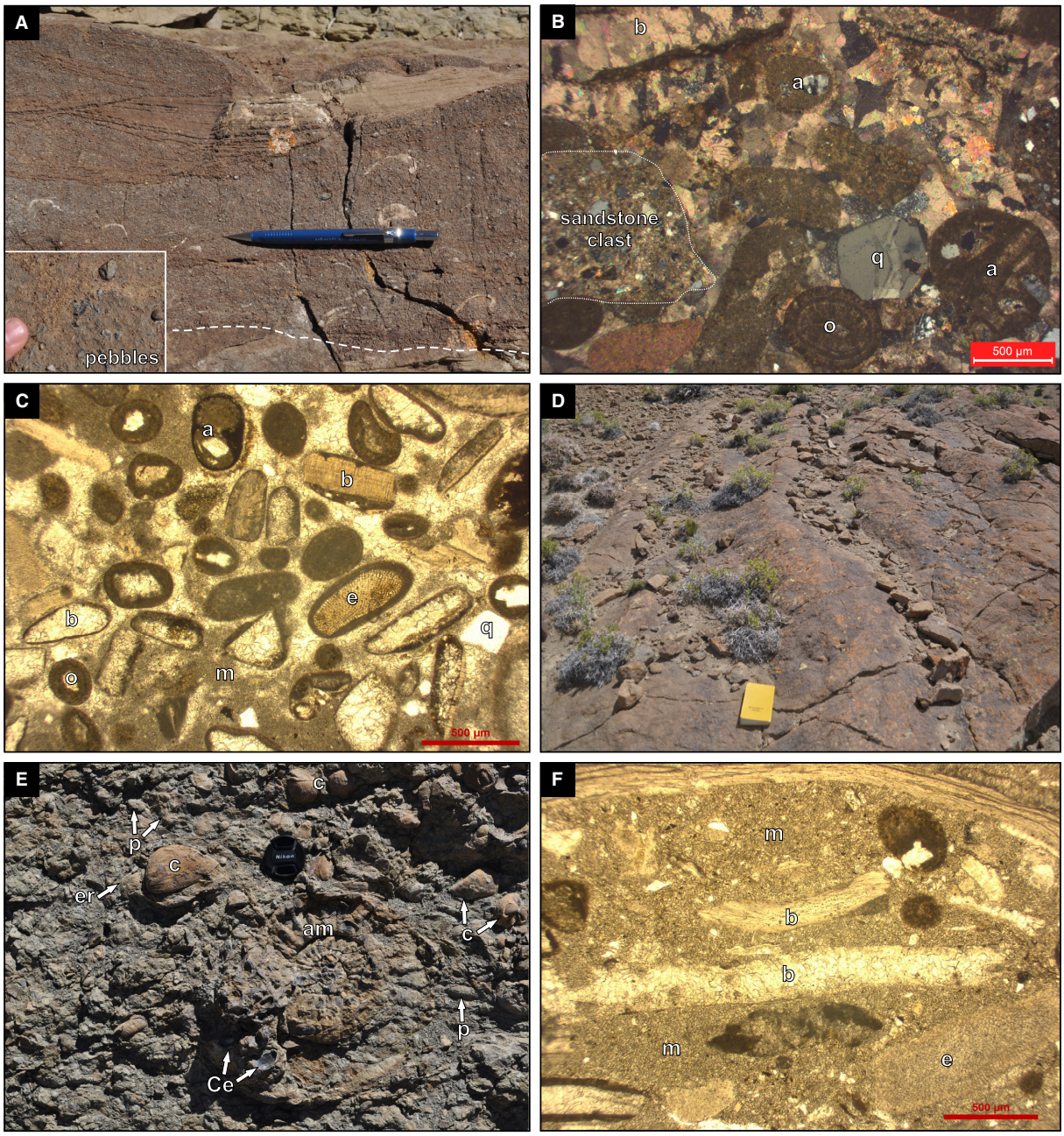

Fig. 8. Main attributes of the shell-bed facies associations. (A) Shoreface shell beds (SSB) showing erosional basal surface (white dashed line) and small-scale trough cross-bedding. Note the concentration of gravel-size bioclasts and terrigenous granules to pebbles (as shown in inset). (B) Thin section photograph (cross-polarized light) of this cross-bedded facies showing the abundance of carbonate grains that characterize these shell beds (bioclasts, ooids and aggregates), together with variable proportions of sandstone, rip-up clasts and siliciclastic coarse-grained material. (C) Thin section photograph (plane-polarized light) of the additional facies included in the SSB facies association. Note the presence of lime mud and lower proportion of siliciclastic material. (D) This muddier facies is typically massive, but the tops can be moulded into large symmetrical ripples that are overlaid (and preserved) by OT or OF deposits. (E) Plan view of the offshore shell-bed (OSB) facies association. This bed is dominated by a high proportion of articulated bivalves belonging to the endobenthic-dominated facies, such as *Cucullaea* sp. (c), *Eriphyla* sp. and *Ptychomya* sp. (p). The epibenthic oyster *Ceratostreon* (Ce) is a subordinate component in this facies, in this example attached to an ammonite (am). (F) Thin section photograph (plane-polarized light) of a bed belonging to OSB. Note the high proportion of carbonate mud and large bioclasts suggesting deposition in low-energy settings and low fragmentation. Legend: a – aggregate; b – bivalve; e – echinoid plate; m – micrite (lime mud); o – ooid; q – quartz. Lens cap is 4·5 cm in diameter, pencil is *ca* 14 cm in length, and field book is 18 cm long.

locally abundant (forming skeletal rudstone) and articulated bivalves are absent. Rip-up clasts of underlying fine-grained sandstone are locally present. The second facies type, which can grade vertically from the previous one, is characterized by skeletal–oolitic packstone, with significant proportion of lime mud (Fig. 8C). In this facies, sand-size grains are associated with abundant and less fragmented gravel-size bioclasts. The fossil association is dominated by oysters and endobenthic bivalves (Table 1), and articulated specimens are locally present. Large symmetrical to slightly asymmetrical ripples are commonly preserved at the top of these carbonate beds (Fig. 8D). In addition to carbonate components, siliciclastic coarse-grained grains and pebbles are commonly concentrated in the two facies (Fig. 8A and B). This facies association overlies LS or US facies associations, and grades vertically to offshore shell beds (described below) or OF and OT facies associations (Fig. 6).

Interpretation

Truncation of underlying sandstone and concentration of coarse siliciclastic and carbonate in thin beds suggest that these shell beds are related to phases of marine erosion and concomitant low supply of terrigenous sand. Additionally, when both facies are present, vertical trends indicate a gradual reduction in hydrodynamic energy. Thus, these shell beds are interpreted as transgressive deposits mantling transgressive ravinement surfaces (Nummedal & Swift, 1987; Naish & Kamp, 1997). The cross-bedded facies, with abundant relict, well-sorted material and lack of mud suggest the generation of transgressive lags (Cattaneo & Steel, 2003) in a shoreface setting with dune development. Conversely, the second facies, with abundant lime mud and large symmetrical ripples, which probably formed by the passage of strong oscillatory flows onto the shelly sea floor (Dumas *et al.*, 2005; Cummings *et al.*, 2009), would suggest a proximal offshore-transition setting (i.e. below but near the fair-weather wave base). In this later facies, shell taphonomy points both to relict fragments, but also new benthic associations that colonized the sea floor during transgression.

Offshore shell beds (OSB)

Description

This association also occurs in thin beds and includes two skeletal-dominated facies, which are characterized by preserved macrofossils surrounded by a lime mud matrix (i.e. skeletal floatstone; Table 1). One end-member facies is dominated by epibenthic bivalves, more commonly cemented oysters (*Ceratostreon* sp.), and the other end member is enriched in endobenthic (shallow-burrowing and deep-burrowing) bivalves (Fig. 8E). When the two facies are in the same stratigraphic interval, the epibenthic-dominated one is replaced northward (i.e. distally) by the other one. Fragments of corals, serpulids, free-lying and endobyssate bivalves and ammonoids are components of both facies. In general, articulation and bioerosion are high in these fossils, whereas fragmentation, orientation of shells and rounding are low. The matrix is dominated by lime mud, with subordinate terrigenous silt and sand-size bioclasts (Fig. 8F). Glauconite is locally common. These shell beds overlie fine-grained deposits of OF or OT facies associations (Fig. 6), and they grade vertically into the BA or OF facies associations.

Interpretation

Taphonomic attributes and composition of fossil associations in both facies suggest parautochthonous to autochthonous assemblages and normal marine salinities (Fürsich, 1995). Shell taphonomy also suggests that all of the macrofossils lived during the generation of the shell beds. The two facies are interpreted to represent a low-energy, well-oxygenated sea floor, characterized by high biogenic carbonate production and minimal terrigenous supply. These shell beds are interpreted to represent offshore conditions and maximum condensation during transgression (Abbott, 1998). Colonization by epibenthic versus endobenthic-dominated communities could have been controlled by rates of carbonate production and sea floor aggradation, as suggested by Schwarz *et al.* (2016b), but other parameters such as nutrient availability and/or water depth could also have played a role.

HIGH-FREQUENCY SEQUENCES (PARASEQUENCES)

Shallowing-upward successions are the dominant motif in the Pilmatué stratigraphy, and they occur at different scales (Figs 5, 9 and 10). Shallowing-upward packages bounded by stratigraphic surfaces that represent abrupt marine flooding are termed parasequences (*sensu* Van Wagoner *et al.*,

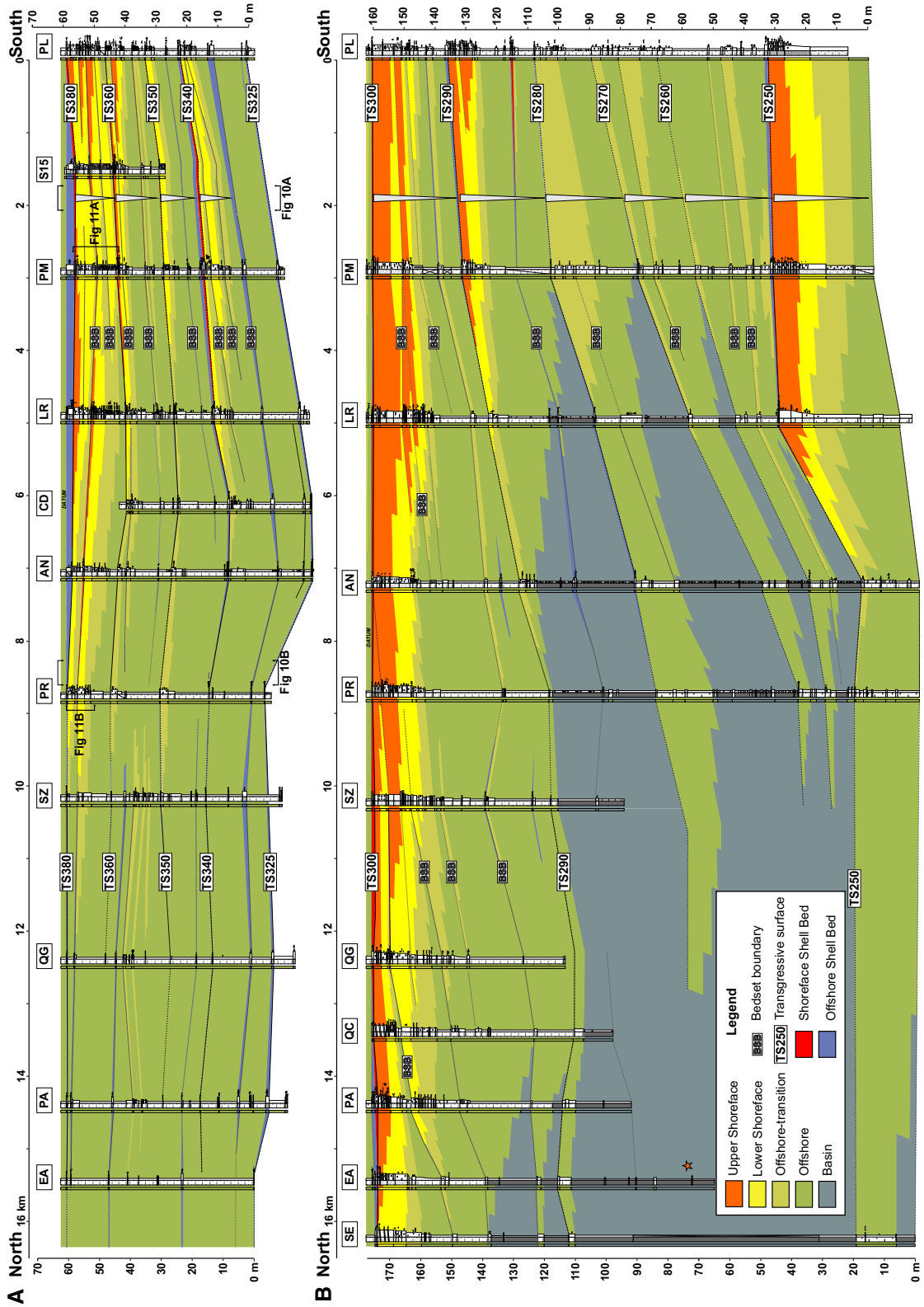

Fig. 9. Detailed cross-sections oriented approximately along depositional dip through two selected intervals of the Pilmatué Member, showing lateral and vertical distribution of facies associations within successive parasequences, shell beds associated with transgressive surfaces and intra-parasequence architecture (bedsets). (A) Study succession from PS250 to PS300. (B) Study succession from PS330 to PS380. Datum is assumed horizontal for simplicity. For log locations, see Fig. 3.

1988), but this definition has an intrinsic problem because it relates to the degree of deepening a surface must show to be defined as such (Catuneanu, 2006; Zecchin & Catuneanu, 2013). In this study, flooding surfaces are consistently defined as those that represent at least a vertical shift of two siliciclastic facies associations in any sector of the study area (i.e. BA deposits overlying OT or shallower deposits, OF deposits overlying LS or US deposits, or OT deposits overlying US deposits). As the stratigraphic units include thin shell beds produced during transgression (Figs 6 and 9), the parasequences identified in this study could be better defined as high-frequency sequences following the Zecchin & Catuneanu (2013) suggestion; but for simplicity, they will be termed parasequences herein. Nonetheless, the bounding surfaces are appropriately defined as transgressive surfaces and placed at the base of the shell beds (Fig. 9A and B).

According to this definition, 17 parasequences were identified in the study interval (Fig. 9; Table 2). These units and their bounding surfaces can be confidently correlated across most of the depositional transect, although precise identification is more difficult in distal areas (Fig. 9). Of the 17 parasequences, 13 record shallowing from BA or OF deposits to LS or US deposits, whereas four document solely shallowing within the distal part of the depositional system (Figs 9 and 10; Table 2). The compacted thickness of completely preserved parasequences ranges from 10 to 50 m (mean of 26 m; Table 2).

Individual parasequences in cases form a single coarsening-upward succession, but more commonly they are composed of bedsets that represent shallowing-upward successions of a higher order (Van Wagoner *et al.*, 1990; Hampson, 2000) (Figs 9 and 11). In this study, the bedset boundaries are surfaces across which there is a minor deepening of the system that is considered as a shift in only one facies association (for example, BA deposits overlying OF deposits and OT deposits overlying OF deposits). Following these criteria, individual parasequences comprise two to six bedsets (Table 2) and bedsets are typically from 5 to 10 m thick. Internally, bedsets show shallowing-upward trends from OF to OT deposits in distal parts of the system (Fig. 9), whereas in proximal parts they comprise OT deposits rapidly passing into LS deposits, and eventually grading to US strata (Fig. 11). Albeit rare, a few bedset boundaries are associated with the presence of shoreface shell beds (Fig. 11B and C), which allow them to be mapped over large distances (for example, PS290 in Fig. 9A; and PS340 and PS380 in Fig. 9B).

PROCESSES, FACIES BELTS AND SHORELINE EVOLUTION

Depositional model

The vertical and lateral relationships between siliciclastic facies associations (OF, OT and LS) and mixed associations (BA and US) of the Pilmatué Member (Fig. 9) allowed reconstruction of the dominant processes and depositional conditions within a siliciclastic-dominated mixed system (Fig. 12A). This system is characterized by a shoreface–basin profile composed of five zones, and is mainly dominated by storm weather and fair-weather wave processes. The basinal setting was characterized by continuous sedimentation of siliciclastic and carbonate mud and by the lack of significant sea floor colonization and/or bioturbation. The latter suggests that reduced oxygen levels at the water–sediment interface and/or lack of nutrients (Fürsich, 1995; Spalletti *et al.*, 2001) were the likely controlling factors inhibiting the development of endobenthic communities. Shoreward, in the offshore setting (Fig. 12A), siliciclastic sedimentation prevailed onto a relatively well-oxygenated sea floor, where bivalves, arthropods and other benthic fauna were able to develop. The fine-grained sediment in this setting could have derived from settling, but its origin could be also related to mud resuspension and the generation of wave-supported sediment gravity flows, a sediment-dispersal process recently recorded in modern shelf systems (Hill *et al.*, 2007; Parson *et al.*, 2007) and described in theoretical studies (Kämpf & Myrow, 2014). In this case, mud resuspension for the Pilmatué system could have occurred associated with the passage of major storms recorded in the offshore-transition zone as discrete storm-event beds.

The offshore-transition setting was dominated by recurrent alternation of siliciclastic mud and sand deposition. Sand was emplaced by combined flows or pure oscillatory flows that moulded the sea floor with large asymmetrical ripples and hummocks under relatively high velocities, and small ripples when flows where less energetic or original flows were waning. This zone was intensely colonized by endobenthic communities producing, in

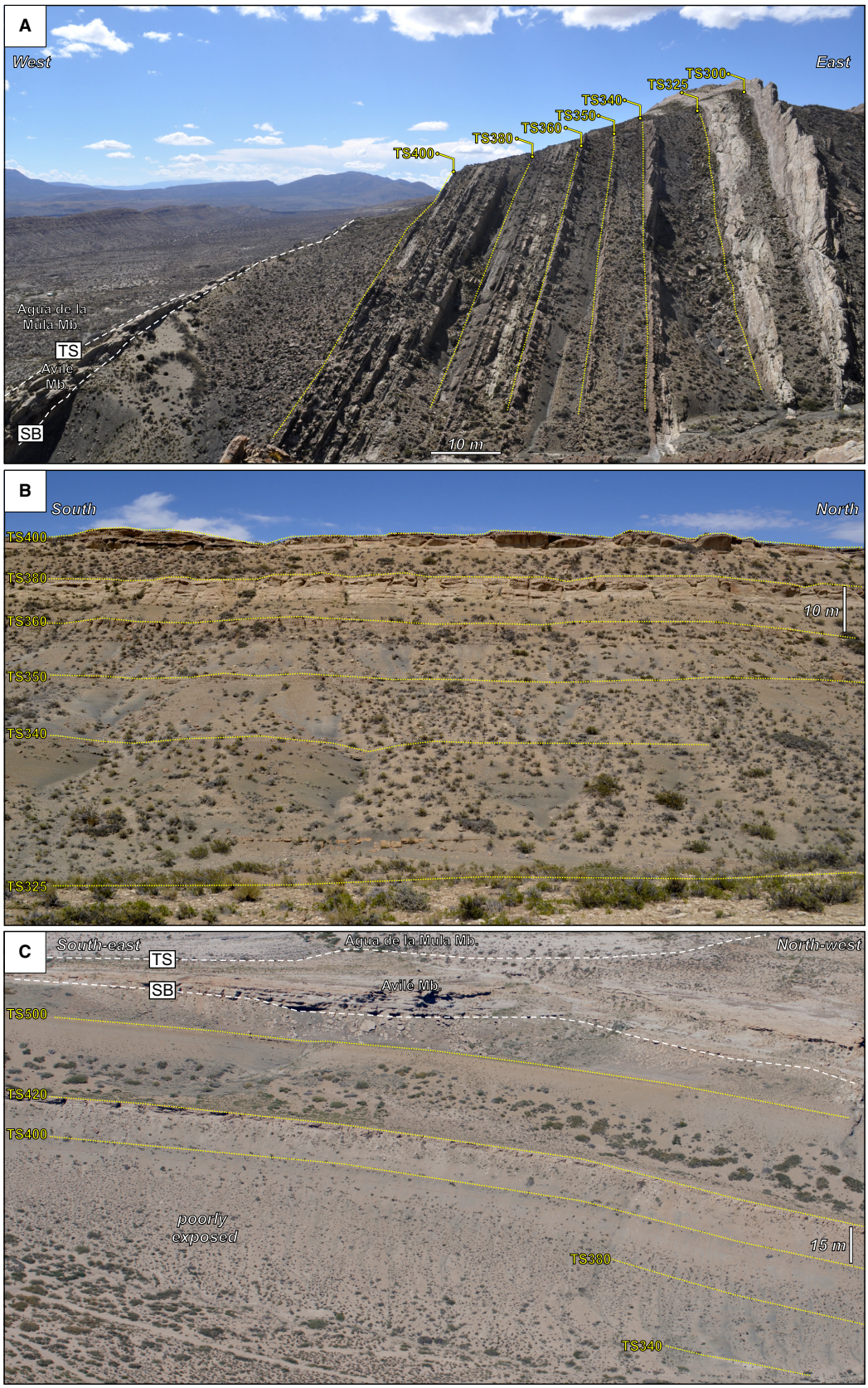

many cases, a complete homogenization of the original heterolithic deposits.

In the lower shoreface setting, the sandy sea floor was mainly mobilized by onshore shoaling waves that produced symmetrical to slightly asymmetrical ripples. These conditions were episodically interrupted by storm-related, combined underflows that generated large asymmetrical ripples and hummocks, as well as plane bed conditions (Dumas *et al.*, 2005; Perillo *et al.*, 2014). Both fair-weather and storm deposits were largely affected by organisms of a *Skolithos* ichnofacies assemblage, suggesting that processes that commonly produce benthic environmental stress, such as high sedimentation rates, turbidity, reduced oxygenation and/or salinity changes (MacEachern *et al.*, 2007b), were not common in this part of the system.

The development and migration of dunes was common in the upper shoreface area, the most landward setting recorded in this depositional model. These dunes probably migrated at a low angle with respect to the reconstructed shoreline orientation (for example, to the north-east for an east–west shoreline), suggesting a significant control of longshore currents and the generation of bar-trough systems in this region (Fig. 12A). Littoral drift was probably responsible for the supply of the siliciclastic sand and subordinate pebbles (see *Discussion* below). The upper shoreface was also an area where contemporaneous mixing of carbonate grains and terrigenous sand took place. Non-skeletal grains (i.e. ooids and aggregates) were probably produced in this region due to high carbonate saturation state and high-energy conditions, as in modern carbonate-dominated ramps and shelves (Gischler & Lomando, 2005; Rankey, 2014) and mixed settings (Michel *et al.*, 2011). However, processes responsible for cross-shelf transport were in general unable to shed siliciclastic and carbonate medium-grained sand (or larger particles) off of the upper shoreface and were consequently stored in that part of the system (Fig. 12A).

Transgressive conditions favoured the formation of extensive shell beds (Fig. 9) that developed on the underlying regressive deposits (Fig. 12B). An exception is sediment in the basinal areas that was never susceptible for benthic colonization; the rest of the sea floor region that was already below fair-weather wave base at the onset of transgression was colonized by bivalve-dominated communities (offshore shell beds). Conversely, the zones that were above fair-weather wave base at the time of transgression underwent erosion and concentration of gravel-size and sand-size material due to wave reworking and ravinement (Nummedal & Swift, 1987; Swift *et al.*, 1991), and high-energy conditions produced well-sorted cross-bedded carbonates (shoreface shell beds; Fig. 12B). Finally, intermediate regions of this carbonate-dominated mixed system favoured the formation of shelly substrates (with variable proportions of lime mud and benthic colonization) in which the passage of storm surges moulded large symmetrical ripples that were occasionally preserved as transgression progressed. Because this contribution focuses on the siliciclastic-dominated mixed depositional system developed during regressive conditions, this transgressive carbonate-dominated system will not be discussed further.

Spatial facies distribution

Coeval sedimentation of carbonate and siliciclastic components in different zones of the regressive part of the Pilmatué depositional system resulted in the development of a mixed, but siliciclastic-rich, storm-dominated environment characterized by three distinctive zones: (i) a mixed distal zone (BA facies association); (ii) a middle siliciclastic zone (OF to LS facies associations); and (iii) a mixed proximal zone (US facies association; Fig. 12A). Moreover, detailed characterization of the facies associations distributions and lateral transitions (Fig. 9) indicates that these zones were individual facies belts that

Fig. 10. Outcrop view of parasequences in proximal, middle and distal sectors of the study area. (A) Proximal setting (between Puesto Mardone and S15 sections) showing the PS300 to PS400 interval. Here, all parasequences contain some proportion of shoreface deposits (B) Middle sector (Riquelme section) showing the PS325 to PS400 interval. Note that shoreface sandstones (whitish sandstones) are only present in PS380 and PS400 parasequences. (C) Distal sector (Puesto Leiva section) showing that the PS325 to P400 interval is here entirely composed of thick offshore mudstone deposits together with thin shell beds. Shoreface deposits are here associated with overlying PS420 and PS500 parasequences. See location of (A) and (B) in Fig. 9B; location of (C) in Fig. 4. TS290 means the transgressive surface of PS290. Legend: SB: – sequence boundary; TS – transgressive surface.

Table 2. Key attributes recognized in the Pilmatué Member parasequences. The number of bedsets typically varies from proximal to distal settings and is shown as a range in the corresponding column. Grey cells indicate no available data; number in italics represents minimum values. TS: transgressive surface; US dunes: upper shoreface dunes; WA: wave approach; SRNSB: storm-reworked nearshore sandstone belt during maximum regression, a parameter defined by Hampson (2010) that combines LS and OT facies belts.

No.	PS	Capping TS	Mean thickness (m)	Facies associations	Number of bedsets	Wave approach and longitudinal currents	Migration direction	Facies-belt width at maximum regression					
								US	LS	OT	OF	BA	SRNSB
1	PS240	240	53	BA, OF, OT	6		NE			4	12	*8*	
2	PS250	250	43	BA, OF, OT, LS, US	3	US dunes to SW	N	5	2	2·5	10	*5*	4·5
3	PS260	260	22	(SSB, OFSB), BA, OF, OT	3		NE			4	8	*12*	
4	PS270	270	16	BA, OF, OT	2		N			5	*7*	*12*	
5	PS280	280	32	(OFSB), BA, OF, OT	2		N			5	8	*11*	
6	PS290	290	22	(OFSB), BA, OF, OT, LS, US	3-2	WA from NNW	N	3·5	2	3	8·5	*7*	5
7	PS300	300	46	(OFSB), BA, OF, OT, LS, US	4	WA from NNW, US dunes to NE	N	16	2	3	*3·5*		5
8	PS310t	N/A	1	SSB, OF, OT, LS	1	WA from NW							
9	PS325	325	1	SSB, OF, OT, LS	1								
10	PS340	340	24	OFSB, OF, OT, LS	4-2	WA from N	N		5	2	*17*		7
11	PS350	350	14	SSB, OFSB, OF, OT, LS	2		N		4	6	*12*		10
12	PS360	360	16	SSB, OFSB, OF, OT, LS, US	3	WA from N	N	4	1·5	6	*10*		7·5
13	PS380	380	14	SSB, OFSB, OF, OT, LS, US	4-2	US dunes to NE	NE	4	2	4	*12*		6
14	PS400	400	32	SSB, OFSB, OF, OT, LS, US	5-2	WA from NNW	N	13	2	3	*6*		5
15	PS420	420	10	SSB, OFSB, OF, OT, LS, US	2-1	WA from SW	W						
16	PS500	500	48	OFSB, OF, OT, LS	1	WA from SW	W		2·5	3	*6*		5·5
17	PS520t	N/A	23	OFSB, OF, OT, LS	4-1	WA from SW, US dunes to NE	W						

were roughly parallel to one another and to the inferred coastline (Fig. 13).

In order to refine the reconstruction of this siliciclastic-dominated mixed system, the width of individual belts was quantified wherever possible (Table 2), by using the up-dip and down-dip pinchouts of individual facies associations at the time of maximum regression, combined with the reconstructed shoreline orientation for each parasequence (Fig. 13). The width of the lower shoreface facies belt varied from 2 to 5 km, whereas the offshore-transition facies-belt width ranged from 2 to 6 km. The combination of these two facies belts (LS and OT) has been defined as the 'storm-reworked nearshore sandstone belt during maximum regression' for pure siliciclastic systems (Hampson, 2010; Hampson *et al.*, 2011). It is possible to estimate the width of this belt for seven parasequences within the study interval (Table 2). The storm-reworked nearshore sandstone belt was *ca* 5 km wide in the lower stratigraphic interval (PS240 to PS300) but increased to 6 to 10 km wide in genetic units of the upper stratigraphic interval (PS340 to PS380). The OF facies belt recorded a similar vertical pattern. It ranges from 7 to 12 km wide in the PS240 to PS290 interval (Table 2), but expanded significantly in the PS340 to PS380 interval, having a minimum width that varied from 10 to 17 km among successive parasequences (Fig. 13).

Shoreline orientation and migration

The overall northward progradation of the Pilmatué Member within the study area (Fig. 4) can be refined using the detailed mapping of individual parasequences (Figs 9 and 10), together with the palaeocurrent analysis for each of those units (Table 2). Integration of these data suggests that the migration direction of the shoreline varied through time (Fig. 13). Northeastward progradation direction is reconstructed for PS240, PS260 and PS380, whereas north-oriented progradation is inferred for most of the parasequences (Fig. 13; Table 2). A significant change occurred in the uppermost interval (PS420, PS500 and PS520). The data suggest that progradation took place mostly from east to west during the development of these parasequences (Figs 4 and 10C), and that only the eastern sector of the study area was located in shoreface conditions (PS500 in Fig. 13).

Within parasequences, the up-dip and down-dip pinchouts of US deposits have been used in previous studies as respective proxies for the initial and final position of the shoreline during progradation (Hampson, 2010; Hampson *et al.*, 2011). The width of the preserved facies belt is therefore an estimation of seaward migration of the shoreline. In this study, the down-dip pinchout of US facies is recorded in six parasequences, but the up-dip pinchout is not

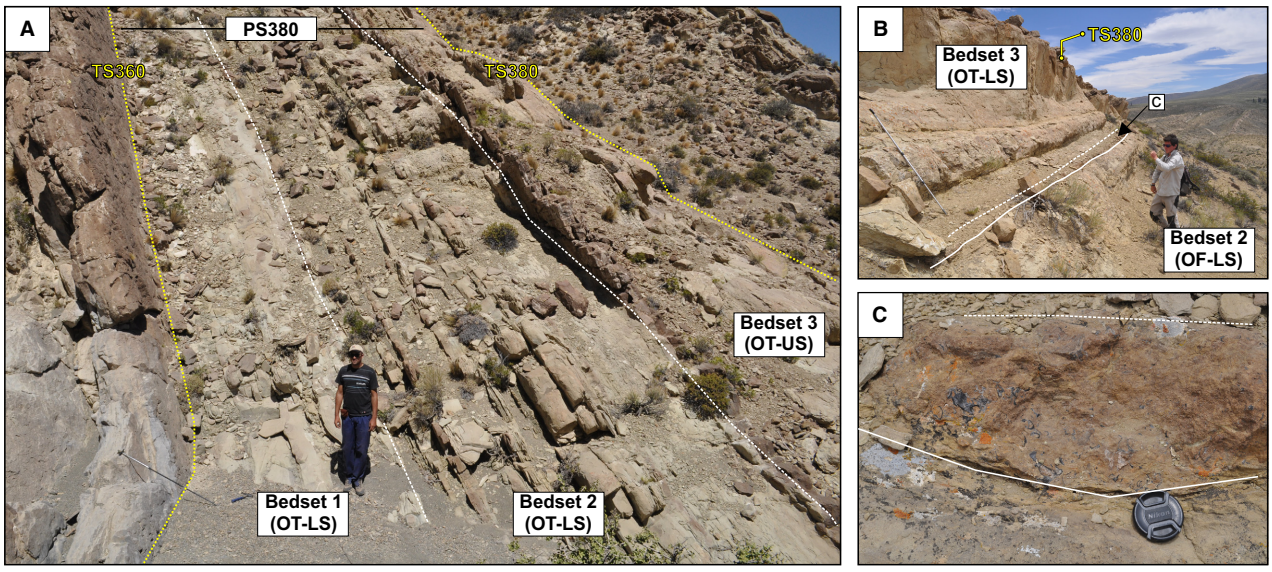

Fig. 11. (A) Internal architecture of parasequences, which are commonly formed by metre thick bedsets. In this example, bounding surfaces (white lines) are typically non-depositional discontinuities representing a minor shift in depositional conditions. (B) and (C) bounding surfaces occasionally demarcated by thin concentration of shells. Persons for scale are *ca* 1·8 m tall. Lens cap is 4·5 cm in diameter.

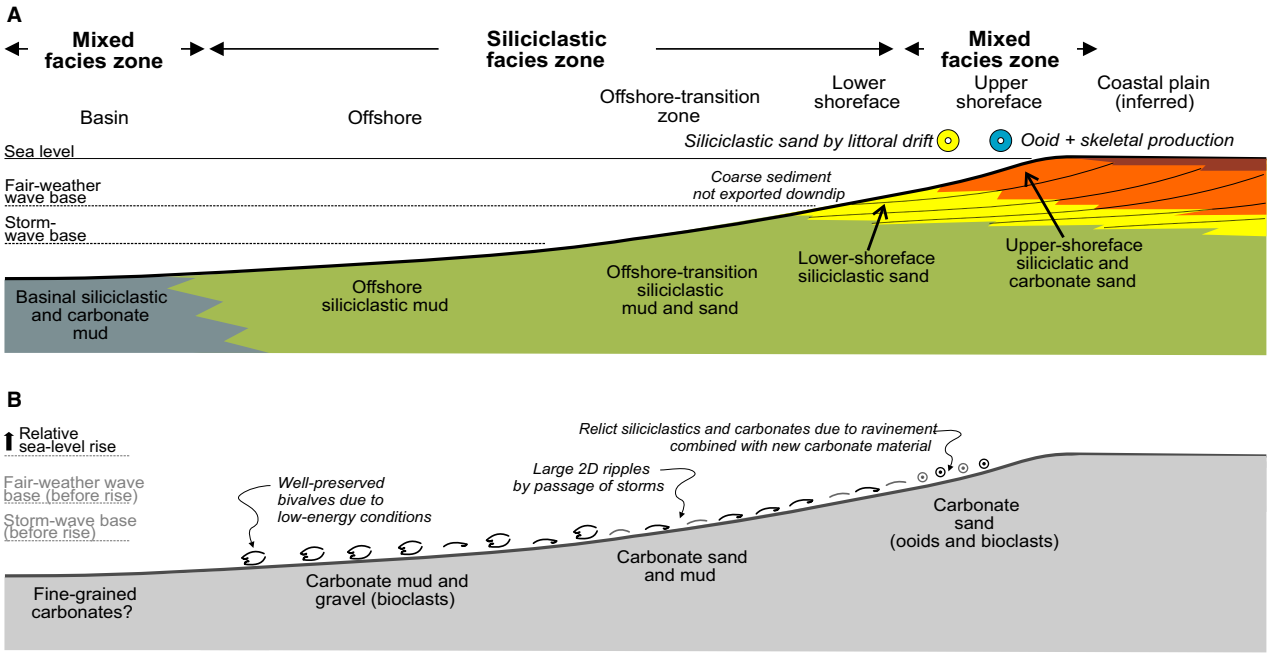

Fig. 12. (A) Storm-dominated and wave-dominated, shoreface–basinal depositional model reconstructed for the early Hauterivian interval on the Pilmatué Member. Coeval mixing of carbonate and terrigenous material occur in the more distal and more proximal zones of the marine system. In the proximal setting, there is a significant contribution of ooids. (B) Simplified, carbonate-dominated system developed during onset of transgression, which favoured the formation of different shell beds across the previous siliciclastic-dominated mixed system.

observed in any of them due to the lack of exposure (or preservation) of coeval coastal plain deposits. Therefore, in this case, the width of the US facies belt is an indication of the minimum value of shoreline progradation (Table 2). The facies belt reaches a maximum width in PS300 and PS400, suggesting a minimum progradation in the order of 16 km and 13 km, respectively (Figs 9 and 13). For the other four parasequences, a minimum progradation of 3 to 6 km has been estimated (Table 2). In the same way, considering the estimated width of different facies belts (Fig. 13; Table 2), transgressive surfaces topping PS250, PS300 and PS400 suggest significant landward displacement of the shoreline, in the order of 10 km for PS250 (Fig. 9), to more than 20 km for PS325.

DISCUSSION

Variability and controls of mixed carbonate–siliciclastic systems

Mixed carbonate–siliciclastic systems have been documented from shallow-marine shelves through most of the Phanerozoic (Table 3). Their configuration and evolution depended heavily on the processes responsible for producing and depositing different types of carbonate grains (i.e. skeletal and non-skeletal), as well as the processes supplying siliciclastic sand and mud to the basins (Coffey & Sunde, 2014; Zeller *et al.*, 2015; Labaj & Pratt, 2016; Schwarz *et al.*, 2016b). Although a wide variety of depositional models (Table 3) and resulting stratigraphic patterns are described for these mixed systems, few published examples have explored the attributes and controls of siliciclastic-dominated mixed systems in which the contribution from non-skeletal carbonates is dominant.

A distinctive feature of the depositional system reconstructed for the Pilmatué Member is the high proportion of non-skeletal (i.e. ooids) grains in the upper shoreface facies belt (Figs 12A and 13). A literature review shows that carbonate-dominated mixed systems are common, but ooid contribution to the carbonate factory is rare (Table 3). Even less common are examples in which ooids were formed and deposited within a siliciclastic-dominated system (Coffey & Sunde, 2014; in Table 3). The modern northern coast of Kuwait (western coast of the Arabian Gulf) has been described as a mixed, siliciclastic-

dominated marine system (Gischler & Lomando, 2005) which is greatly influenced by the siliciclastic input from the Euphrates and Tigris rivers. However, the terrigenous contribution decreases rapidly southward, and most of the coast of Kuwait becomes a carbonate-dominated system with a high proportion of ooids being generated in the high-energy inner ramp (Gischler & Lomando, 2005; see Table 3). Another example is located in north-western Africa, where Michel *et al.* (2011) reported the formation of aragonite ooids in isolated bays along the coast of Mauritania, which are mixed in shallow waters (<20 m) with aeolian-derived siliciclastic material and skeletal fragments. Hydrodynamic studies on how the sediment is being mixed in this marine environment, and resulting facies belts patterns, are not available.

In any case, it is worth noting that these two examples of siliciclastic-dominated mixed systems are developed in shallow seas associated with arid continental conditions, where river discharge and sediment supply are associated with isolated entry points, leaving tens to hundreds of kilometres of the remaining shoreline without direct sediment input. Because the Neuquén Basin was a shallow epeiric sea (Howell *et al.*, 2005) located in an arid climate belt during the Early Cretaceous (Scotese, 2000), it is plausible that these conditions could have favoured the development of a similar siliciclastic-dominated, mixed system, away from the major source of siliciclastic supply to the basin. The non-skeletal carbonate production (i.e. ooid formation) could have been aided by the arid climate and the greenhouse conditions that prevailed during the Hauterivian (Föllmi, 2012). In this context, the lack of studies reporting modern mixed systems similar to that inferred for the Pilmatué Member (Table 3) could be due to a bias towards the study of mixed, but carbonate-dominated systems, or a result of the low occurrence of these systems at present.

Siliciclastic-dominated mixed systems versus pure siliciclastic systems

Except for the concurrent contribution of ooids and siliciclastic sand to the upper shoreface, the dominant depositional processes and facies belts reconstructed for the siliciclastic-dominated mixed system of the Pilmatué Member (Figs 12A and 13) do not differ from well-known, shoreface to shelf depositional systems developed in pure siliciclastic marine systems (Walker & Plint, 1992; Reading & Collinson, 1996). Both systems are characterized by storm and fair-weather related transport and deposition, and by the formation of facies belts that are mainly parallel to the shoreline. As a consequence, high-frequency sequences in the Pilmatué Member, and the inferred short-term evolution of shoreline migration (Figs 9 and 13; Table 2), are also markedly similar to the parasequences developed in purely siliciclastic systems (Walker & Plint, 1992; Reading & Collinson, 1996; Hampson & Storms, 2003). Bedsets, a main component of parasequences in siliciclastic systems (Van Wagoner *et al.*, 1990; Hampson, 2000; Hampson *et al.*, 2011; Zecchin *et al.*, 2017), are also common in the siliciclastic-dominated, mixed system reconstructed in this study (Figs 9 and 12A).

The large-scale palaeogeographic scenario reconstructed for the siliciclastic-dominated, mixed system of the Pilmatué Member can also be compared with pure siliciclastic-dominated systems. Due to the arid conditions, large extensions of the shoreline provided little volume of terrigenous sand via direct fluvial entry points, but relatively large and coeval deltaic systems have been reported recently from subsurface data (Schwarz *et al.*, 2016c), located to the south of the study area (Fig. 14). Thus, it is inferred that most of the siliciclastic sand that was deposited in the Pilmatué shoreface system was sourced by littoral drift from these deltas, associated with major fluvial systems. This hypothesis is also supported by the predominant north-east directed longshore palaeocurrents identified for several parasequences (Fig 13; Table 2). This reconstruction of the Pilmatué Member is analogous to several modern examples in which longshore sand drift provides siliciclastic sediment to form strandplains and barriers in a down-drift direction (Curray *et al.*, 1969; Anthony & Blivi, 1999). It is also similar to that generated for an ancient pure siliciclastic example (Ksp40-Panther Tongue of Hampson *et al.*, 2011). Thus, it is reasonable to suggest that long-term evolution and, ultimately, controls on stratal architecture could be similar in both shoreface–shelf pure siliciclastic systems and the siliciclastic-dominated end of mixed systems. For example, the change in local palaeogeography and shoreline migration that is recorded in the uppermost parasequences (rotation of 90° from an east–west orientation to a more north–south orientation; see PS500 in

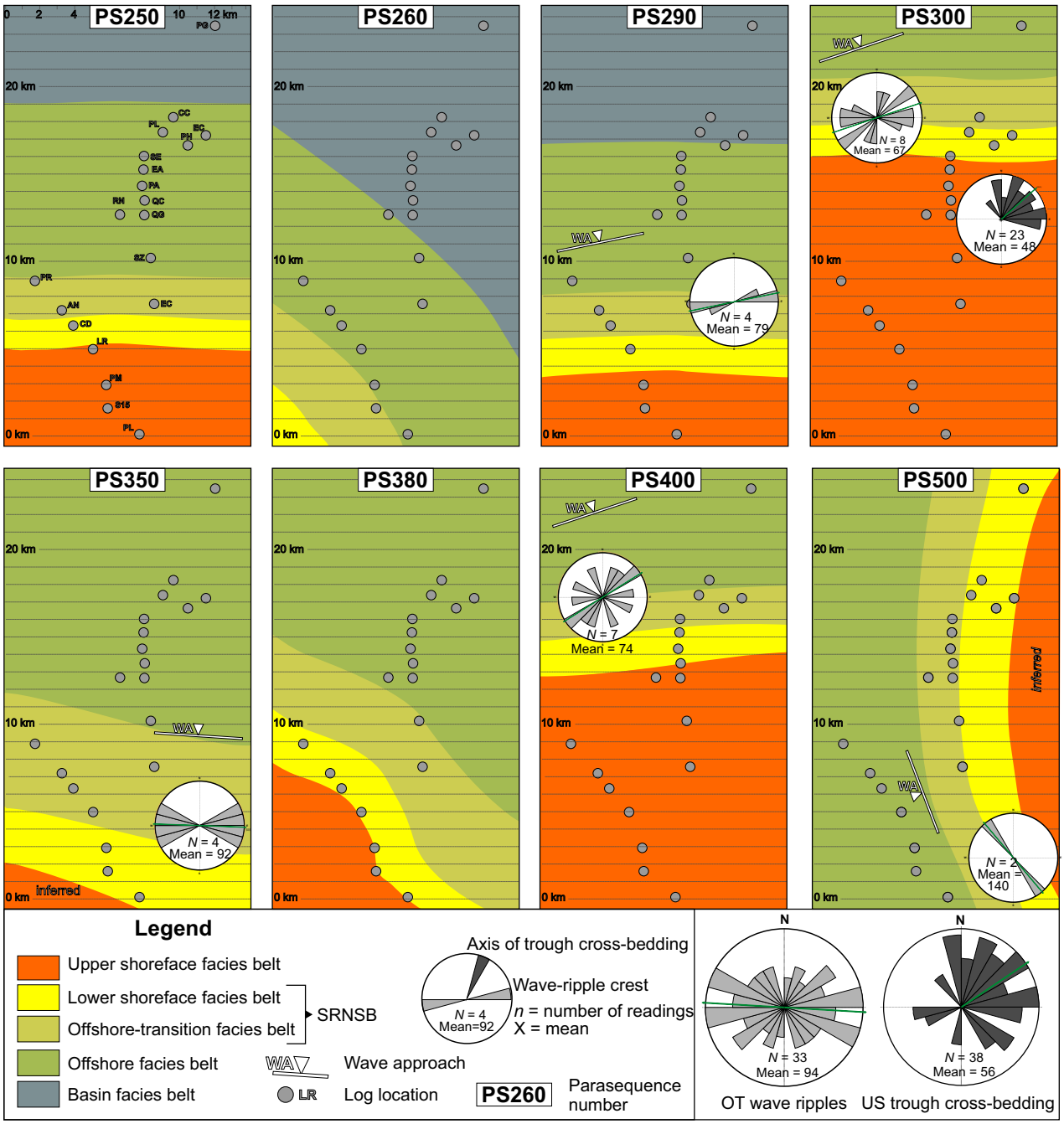

Fig. 13. Facies belt reconstructions for selected parasequences of the Pilmatué Member in the study area. The reconstruction considers the uppermost distribution of deposits (and therefore facies belts), prior to transgressive conditions (see text for more explanation). SRNSB: storm-reworked nearshore sandstone belt during maximum regression. When possible, palaeocurrent data for OT wave ripple crests and US trough cross-bedding are also provided for each parasequence. The compilation of palaeocurrent data associated with these attributes for the entire succession is also presented (inset).

Fig. 13) could be described as a large-scale rotational event, as recently reported for some nearshore Cretaceous successions (Madof *et al.*, 2015). This shoreline rotation event, as in pure siliciclastic systems, could have been triggered by different mechanisms such as tectonic forcing, changes in the overall sand volume supplied by deltaic systems to the basin and/or the transport efficiency of the existent littoral drift (Fig. 14).

One basin, one climate regime, different types of mixed systems

Examples of ancient mixed carbonate–siliciclastic systems include both icehouse and greenhouse climatic regimes (Table 3). Even within one climatic mode, mixed systems can be highly variable, especially if factors such as siliciclastic transport processes and carbonate factories vary in space and time (Table 3). The Neuquén Basin, which includes Upper Jurassic to Lower Cretaceous mixed carbonate–siliciclastic successions, provides an opportunity to explore the wide range of mixed systems that can be generated within a single basin and under relatively uniform climatic conditions.

Mixed carbonate–siliciclastic systems in the Neuquén Basin have been recognized for many years (Groeber, 1946; Legarreta & Uliana, 1991; Spalletti *et al.*, 2000, 2001), but few studies have attempted to reconstruct them in detail across their depositional dip. Recently, Zeller *et al.* (2015) reviewed the depositional conditions and controls of the Tithonian–Berriasian mixed depositional system (Vaca Muerta–Picun Leufú–Quintuco system). These authors concluded that during progradation (i.e. highstand), this gently inclined shelf was a mixed system, with a prevailing carbonate factory in the inner shelf providing ooids and skeletal fragments to form pure carbonate (Fig. 15A). High-energy, ooid-rich bodies were mostly detached from the shoreline and probably deposited under tide-related currents. In the outer shelf and gentle slope, along-shelf currents were responsible for bringing terrigenous silt and very fine sand from remote regions, producing mixed facies belts. However, because these currents were of low efficiency during highstand conditions due to the relative low depth for them to operate (Zeller *et al.*, 2015), siliciclastic supply was comparatively low at that time and a mixed, but carbonate-dominated, system developed (Fig. 15A). Additionally, Zeller *et al.* (2015) suggested that terrigenous supply to the system was higher during lowstand and transgressive intervals due to more efficient distribution of along-shelf currents, which resulted in genetic units (high-frequency cycles and sequences) with siliciclastic-dominated, lowstand and transgressive sediments (Fig. 15A).

In marked contrast, the shallow-marine system of the Pilmatué Member was mixed, but siliciclastic-dominated during regressive conditions (Fig. 15B). High-energy, mixed deposits were attached to the shoreline and resulted from the mixing of siliciclastic sediment supplied mostly by littoral drift (from the south; Fig. 14), and biogenic and non-biogenic carbonate production. Furthermore, the inability of storm-surge flows to export relatively coarse carbonate offshore produced siliciclastic facies belts in the middle zone of the system (Fig. 15B). The upper intervals of parasequences reported in this study are enriched in high-energy mixed sediments, but only if upper shoreface deposits are present. Therefore, the presence of mixed facies is dependent on the facies-belt distribution and cannot be related to temporal changes in the efficiency of along-shelf currents to supply terrigenous sediment to the system, as proposed by Zeller *et al.* (2015) for the Tithonian–Berriasian system. Moreover, the basal intervals of parasequences in the Pilmatué Member are associated with maximum carbonate concentration and shell-bed generation, and these are interpreted to be related to sediment starvation during shoreline transgression (Fig. 15B). As a result, the sequential architecture of genetic units in each case is markedly different.

This comparison highlights the complexity that mixed systems, even within the same basin and with similar climate regime, can produce (Fig. 15). The general proportion of carbonate production with respect to siliciclastic supply, combined with dominant marine transport processes (for example, along-shelf currents, storm-related cross-shelf flows and longshore currents) can create a variety of mixed systems, ranging from carbonate-dominated to siliciclastic-dominated (Table 3).

Reservoir implications

The present study, by expanding the spectrum of mixed systems towards the siliciclastic-dominated end, provides new insights for conventional and unconventional hydrocarbon exploration in these highly complex systems. This can be especially significant for the prediction on composition, geometry and location of high-energy facies in conventional exploration, as well as the composition of the distal fine-grained rocks in an unconventional reservoir.

Oolitic–skeletal bodies in carbonate-dominated mixed systems, such as that reconstructed in

Table 3. Case studies of mixed carbonate–siliciclastic systems, ordered from the carbonate-dominated end (top) to the siliciclastic-dominated end (bottom) of the expected spectrum (this work). For those case studies where different mixed regressive and transgressive systems are reported (Coffey & Sunde, 2014), only the regressive system is considered for comparison. Location, age, climate regime, depositional setting, source of siliciclastic sediments, dominant carbonate factory and cross-shelf transport are provided in each case, together with a schematic reconstruction of the depositional system.

CASE STUDY	LOCATION	AGE	CLIMATE/ CLIMATE REGIME	DEPOSITIONAL SETTING	SOURCE OF SILICICLASTICS	CARBONATE FACTORY	CROSS-SHELF TRANSPORT	FACIES BELT COMPOSITION	SCHEMATIC RECONSTRUCTION OF MIXED SYSTEM (P M D)
Guischer & Lomando (2005)	NW Persian Gulf, Kuwait	Holocene	Tropical & Arid/ Icehouse	Ramp, Interior Sea	Aeolian + Longshore currents	Heterozoan + Ooids	Wave energy, storm-related currents?	Inner Ramp: M/C Middle and Outer Ramp: C Basin: M	
Zeller *et al.* (2015)	Neuquén Basin, Argentina	Late Jurassic-Early Cret.	Temperate & Arid/ Greenhouse	Gentle shelf, Epeiric sea	Along-shelf currents	Heterozoan + Ooids	Tidal/Shelf-related curents	Nearshore and Inner Shelf: C Middle and Outer Shelf: M	
Sanders & Höfling (2000)	Northern Calcareous Alps, Austria	Late Cretaceous	Tropical & Temperate/ Greenhouse	Shelf	Along-shelf currents	Heterozoan + Photozoan	Limited	Nearshore: C Middle Shelf: M Middle Shelf to Outer Shelf: S	
Purdy & Gischler (2003)	Barrier Reef, Belize	Holocene	Tropical & Semiarid/ Icehouse	Shelf	Local fluvial entry points	Photozoan	Limited	Nearshore: S/M Lagoon: M Lagoon to Reef Barrier: C	
Coffey & Read (2007)	Albemarle Basin, USA	Palaeogene	Tropical & Temperate/ Icehouse	Distally steepened ramp	Local fluvial entry points	Heterozoan	Storm-related currents	Nearshore: S/M Inner Shelf: C Outer Shelf: C/M	
Labaj & Pratt (2016)	South-Central Arizona, USA	Middle-Late Cambrian	Equatorial & Humid?/ Greenhouse	Ramp, Epeiric sea	N/A	Heterozoan + Ooids	Storm-related currents	Nearshore: S Offshore-Transition: C Offshore: M	
D´Agostini *et al.* (2015)	Abrolhos Shelf, Brazil	Pleistocene-Holocene	Tropical/ Icehouse	Shelf	Local fluvial entry points + Longshore currents	Photozoan + Heterozoan	N/A	Inner Shelf: S Middle Shelf: M Outer Shelf: C	
Coffey & Sunde (2014)	Albemarle Basin, USA	Early Cretaceous	Tropical & Humid/ Greenhouse	Shelf	Local fluvial entry points + Longshore currents	Heterozoan + Ooids	Storm-related currents	Nearshore: S Offshore-Transition: M Offshore: S Basin: M	
This work	Neuquén Basin, Argentina	Early Cretaceous	Temperate & Arid/ Greenhouse	Ramp, Epeiric sea	Longshore currents	Ooids + Heterozoan	Storm-related currents	US: M LS+OT+OF: S Basin: M	

CARBONATE-DOMINATED

SILICICLASTIC-DOMINATED

System Sectors
P Proximal
M Middle
D Distal

Source of Siliciclastics
Aeolian input
Local Fluvial input
Longshore input
Along-shelf input

Carbonate Factory & Location
Heterozoan
Photozoan
Ooids

Facies belt composition
Pure siliciclastic (S) — Mixed sediments (M) — Pure carbonate (C)

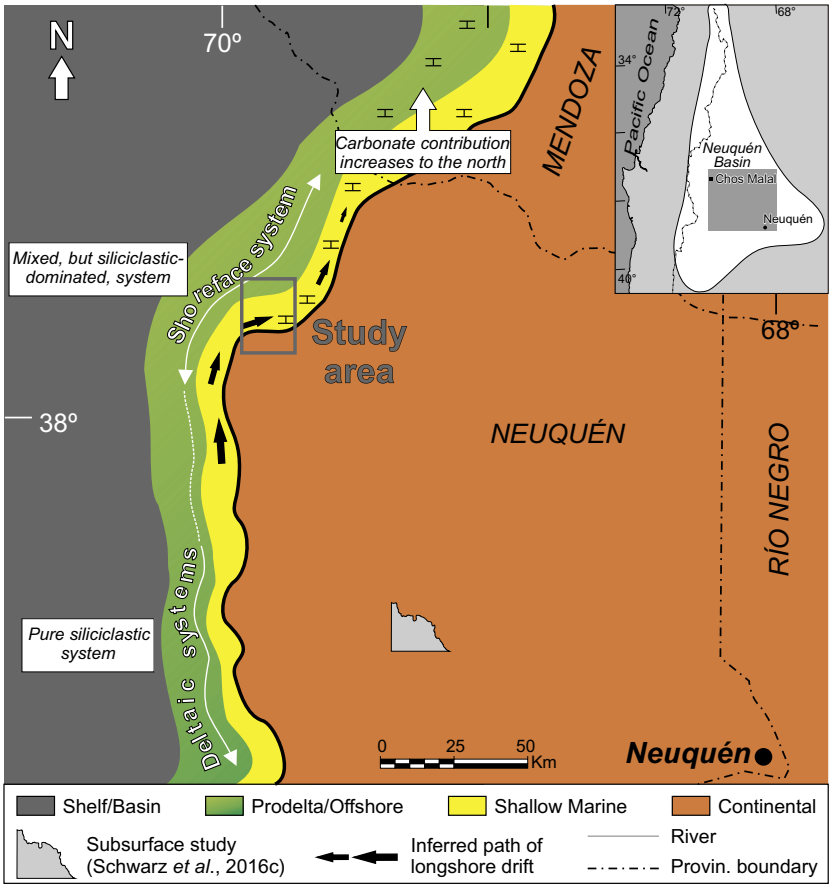

Fig. 14. Large-scale palaeogeographic reconstruction (without palimpsestic restoration) inferred for the Pilmatué Member, showing deltaic systems recognized in the southern sector of the basin. These river-influenced, deltaic systems (and maybe others yet to be recognized) most probably provided siliciclastic sand and mud to the shoreface-basin system developed in the study area.

Fig. 15A, would have an elongated geometry oriented parallel to prevailing tidal currents. These bodies would be developed in shelf regions detached from the coeval shoreline and surrounded by non-reservoir muddier facies. In marked contrast, similar facies in the Pilmatué Member would conform wedge-shape bodies located near the shoreline and oriented parallel to it (i.e. mixed upper shoreface deposits in Fig. 15B). Internal (depositional) heterogeneity would be comparatively low, and these bodies would pass laterally into pure siliciclastic lower shoreface sandstones.

Fine-grained sediments in distal sectors of mixed systems can result from combination of carbonates (both biogenic and exported) and fine-grained siliciclastics brought by along-shelf currents (Fig. 15A). In that situation, a lateral trend characterized by an increment of carbonate contribution towards the proximal part of the system would be expected. Conversely, in mixed systems where fine-grained siliciclastics are transported distally by across shelf processes (Fig. 15B), the carbonate contribution would increase towards the distal most part of the system. Because the mineralogy of mudstone rocks exerts a strong control in several processes, such as organic matter conversion, expulsion of hydrocarbons, petrophysical properties and geomechanical attributes of unconventional reservoirs (Patterson & Henstridge, 1990; Patterson *et al.*, 1990), understanding the composition of the fine-grained rocks in distal sectors of a mixed system and the expected lateral trends could be key results to predict lateral variability of reservoir properties in analogous unconventional reservoirs.

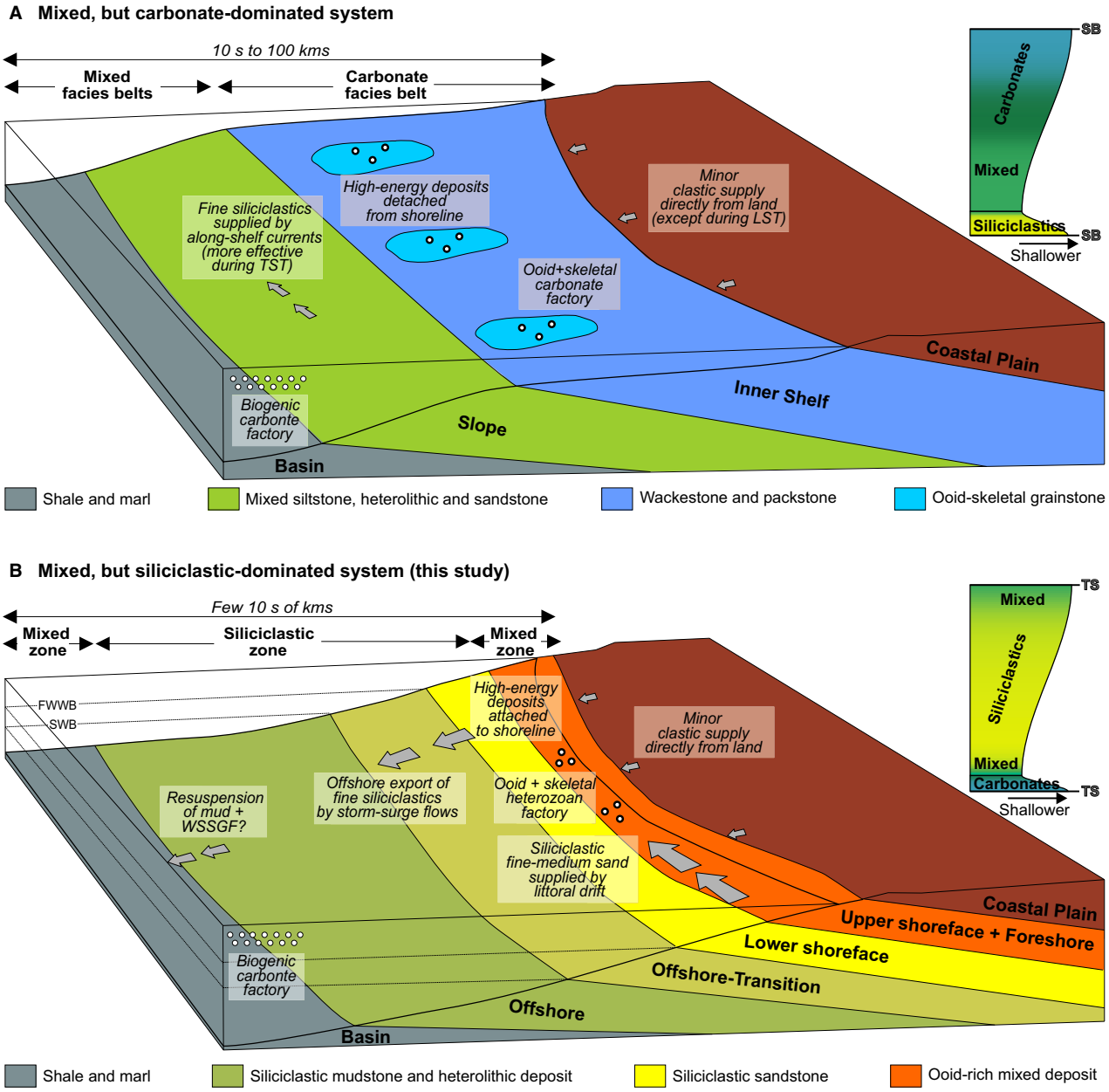

Fig. 15. Contrasting regressive shallow-marine mixed systems. (A) Carbonate-dominated mixed system based on the Tithonian–Berriasian succession of the Neuquén Basin (after Zeller *et al.*, 2015). (B) Siliciclastic-dominated mixed system reconstructed for the Pilmatué Member in this study. Distribution of pure siliciclastic, mixed and/or pure carbonate facies belts varies between systems, resulting in different sequence architecture of stratigraphic units. Note the different horizontal scale between systems. Coastal plain deposits are inferred in both examples. Colour of siliciclastic, mixed and carbonate sediments used in genetic units as in Table 3. Legend: WSSGF – wave-supported sediment gravity flows; TST – transgressive systems tract; LST – lowstand systems tract; SB – sequence boundary; TS – transgressive surface.

CONCLUSIONS

Based on the detailed sedimentological analysis of the early Hauterivian interval of the Pilmatué Member in a 25 km long and 300 m thick outcrop, the following conclusions are drawn:

1 A storm-dominated, shoreface–basinal depositional system comprising three parallel zones was developed during progradation: (i) a mixed distal zone (basin facies association); (ii) a middle siliciclastic zone (offshore to lower shoreface facies associations); and (iii) a mixed proximal

zone (upper shoreface facies association). Thus, the strata record a mixed, but siliciclastic-dominated system. The estimation of the width for the offshore (7 to 12 km), offshore-transition (3 to 6 km) and lower shoreface (2 to 5 km) facies belts provided additional geomorphological information for the system.

2 In this siliciclastic-dominated mixed system, terrigenous sediment was mostly supplied via along-shore currents to the upper shoreface (probably from deltaic systems located to the south), where they mixed with ooids and bioclasts derived from a heterozoan factory. Storm-surge flows were the major mechanisms for across shelf transport, exporting fine sand and mud offshore. Terrigenous and carbonate medium-grained (and coarser) sediments were stored in the upper shoreface. The distal zone received low volumes of siliciclastics, which mixed with planktonic-derived carbonate material.

3 Seventeen parasequences (10 to 50 m thick) bounded by transgressive surfaces and composed of two to six bedsets (5 to 10 m thick) were identified in the study interval. Each parasequence represents up to 16 km of preferentially northward or north-eastward shoreline progradation, but with a significant change to westward progradation in the uppermost three parasequences. Landward migration of the shoreline during transgression favoured the formation of extensive shell beds associated with shoreface erosion and lag generation, as well as offshore condensation. Landward displacement of up to 20 km was estimated.

4 The inferred depositional model and resulting genetic units of the Pilmatué Member siliciclastic-dominated mixed system are markedly different from most carbonate-dominated mixed systems, even for examples developed in the same basin and under a similar climate regime.

5 Conversely, this siliciclastic-dominated mixed system resembles the storm-influenced and wave-influenced siliciclastic counterpart in several attributes, such as depositional processes, internal architecture of parasequences and regional palaeogeographic scenarios.

6 Basin-scale controls, such as arid climatic conditions and the development of a shallow epeiric sea, might help development of mixed systems across the full carbonate–siliciclastic spectrum. The interplay of processes that supply sand to the system, as well as processes transporting sediment offshore across the marine environment, are key controls in shaping the facies distribution and the genetic units of siliciclastic-dominated mixed systems.

7 Reservoir characteristics (geometry, distribution, heterogeneities, etc.) of conventional and unconventional facies would be strongly dependent on the type of mixed carbonate–siliciclastic system. In the regressive Pilmatué Member, proximal high-energy, mixed facies are subparallel and attached to the coeval shoreline, whereas distal fine-grained facies show a seaward increment in carbonate contribution.

ACKNOWLEDGEMENTS

The authors would like to thank CONICET (Consejo Nacional de Investigaciones Científicas y Técnicas), Universidad Nacional de La Plata and YPF S.A. for financial support of this project. José Luis Burini and Agustín Argüello are thanked for field and laboratory assistance. The manuscript benefitted from constructive reviews by C. Di Celma, J. Kosse, P. Myrow and S. A. Abott, as well as additional comments by Associate Editor C. Fielding.

REFERENCES

Abbott, S.T. (1998) Transgressive systems tracts and onlap shellbeds from middle-Pleistocene sequences, Wanganui Basin, New Zealand. *J. Sed. Res.*, **68**, 253–268.

Aguirre-Urreta, M.B., **Rawson, P.F.**, **Concheyro, G.A.**, **Bown, P.R.** and **Ottone, E.G.** (2005) Lower Cretaceous biostratigraphy of the Neuquén Basin. In: *The Neuquén Basin, Argentina: A Case Study in Sequence Stratigraphy and Basin Dynamics* (Eds G. Veiga, L. Spalletti, J. Howell and E. Schwarz), Geol. Soc. London Spec. Publ., **252**, 57–81.

Aguirre-Urreta, M.B., **Lazo, D.G.**, **Griffin, M.**, **Vennari, V.**, **Parras, A.M.**, **Cataldo, C.**, **Garberoglio, R.** and **Luci, L.** (2011) Megainvertebrados del Cretácico y su importancia bioestratigráfica. In: *Geología y Recursos Naturales de la Provincia del Neuquén* (Eds H. Leanza, J. Vallés, C. Arregui and J. C Danieli). pp. 465–488. Relatorio del XVIII Congreso Geológico Argentino, Buenos Aires.

Anthony, E.J. and **Blivi, A.B.** (1999) Morphosedimentary evolution of a delta-sourced, drift-aligned sand barrier-lagoon complex, western Bight of Benin. *Mar. Geol.*, **158**, 161–176.

Arnott, R.W.C. (1993) Quasi-planar-laminated sandstone beds of the Lower Cretaceous Bootlegger Member, North-Central Montana: evidence of combined-flow sedimentation. *J. Sed. Petrol.*, **63**, 488–494.

Cantalamessa, G., **Di Celma, C.** and **Ragaini, L.** (2005) Sequence stratigraphy of the Punta Ballena member of the Jama Formation (Early Pleistocene, Ecuador): insights from integrated sedimentologic, taphonomic and paleoecologic analysis of molluscan shell concentrations. *Palaeogeogr. Palaeoclimatol. Palaeoecol.*, **216**, 1–25.

Cattaneo, A. and **Steel, R.J.** (2003) Transgressive deposits, a review of their variability. *Earth-Sci. Rev.*, **62**, 187–223.

Catuneanu, O. (2006) *Principles of Sequence Stratigraphy*. Elsevier, Amsterdam, 375 pp.

Clifton, H.E. (2006) A re-examination of facies models for clastic shorelines. In: *Facies Models Revisited* (Eds H.W. Posamentier and R.G. Walker), SEPM Spec. Publ., **84**, 293–337.

Coffey, B.P. and **Read, J.F.** (2007) Subtropical to temperate facies from a transition zone, mixed carbonate-siliciclastic system, Palaeogene, North Carolina, USA. *Sedimentology*, **54**, 339–365.

Coffey, B.P. and **Sunde, R.F.** (2014) Lithology-based sequence-stratigraphic framework of a mixed carbonate-siliciclastic succession, Lower Cretaceous, Atlantic coastal plain. *AAPG Bull.*, **98**, 1599–1630.

Cummings, D.I., **Dumas, S.** and **Dalrymple, R.W.** (2009) Fine-grained versus coarse-grained wave ripples generated experimentally under large-scale oscillatory flow. *J. Sed. Res.*, **79**, 83–93.

Curray, J.R., **Emmel, F.J.** and **Crampton, P.J.S.** (1969) Holocene history of a strand plain, lagoonal coast, Nayarit, Mexico. In: *Coastal Lagoons, a Symposium* (Eds A.A. Castañares and F.B. Phleger), pp. 63–100. University Nacional Autonoma Mexico–UNESCO, Mexico.

D'Agostini, D.P., **Bastos Cardoso, A.** and **Dos Reis, A.T.** (2015) The modern mixed carbonate-siliciclastic Abrolhos shelf: implications for a mixed depositional model. *J. Sed. Res.*, **85**, 124–139.

Digregorio, J.H. and **Uliana, M.A.** (1980) Cuenca Neuquina. In: *Geología Regional Argentina* (Ed. J.C.M. Turner), Academia Nacional de Ciencias, Córdoba, **2**, 985–1032.

Dumas, S., **Arnott, R.W.C.** and **Southard, J.B.** (2005) Experiments on oscillatory-flow and combined flow bed forms: implications for interpreting parts of the shallow marine rock record. *J. Sed. Res.*, **75**, 501–513.

Föllmi, K.B. (2012) Early Cretaceous life, climate and anoxia. *Cretaceous Res.*, **35**, 230–257.

Fürsich, F.T. (1995) Approaches to the palaeoenvironmental reconstructions. *Geobios*, **18**, 183–195.

Gischler, E. and **Lomando, A.J.** (2005) Offshore sedimentary facies of a modern carbonate ramp, Kuwait, northwestern Arabian-Persian Gulf. *Facies*, **50**, 443–462.

Goldhammer, R.K. (2003) Cyclic sedimentation. In: *Encyclopedia of Sediments and Sedimentary Rocks* (Eds G.V. Middleton, M.J. Church, M. Coniglio, L.A. Hardie and F.J. Longstaffe), pp. 271–293. Springer, Netherlands.

Groeber, P. (1946) Observaciones geológicas a lo largo del meridiano 70°. 1. Hoja Chos Malal. *Rev. Soc. Geol. Argentina*, **1**, 177–208.

Hampson, G.J. (2000) Discontinuity surfaces, clinoforms, and facies architecture in a wave-dominated, shoreface-shelf parasequence. *J. Sed. Res.*, **70**, 325–340.

Hampson, G.J. (2010) Sediment dispersal and quantitative stratigraphic architecture across an ancient shelf. *Sedimentology*, **57**, 96–141.

Hampson, G.J. and **Storms, J.E.A.** (2003) Geomorphological and sequence stratigraphic variability in wave-dominated, shoreface-shelf parasequences. *Sedimentology*, **50**, 667–701.

Hampson, G.J., **Royhan Gani, M.**, **Sharman, K.F.**, **Irfan, N.** and **Bracken, B.** (2011) Along-strike and down-dip variations in shallow-marine sequence stratigraphic architecture: upper Cretaceous Star Point Sandstone, Wasatch Plateau, Central Utah, U.S.A. *J. Sed. Res.*, **81**, 159–184.

Hill, P.S., **Fox, J.M.**, **Crockett, J.S.**, **Curran, K.J.**, **Friedrichs, C.T.**, **Rockwell Geyer, W.**, **Milligan, T.G**, **Ogston, A.S.**, **Puig, P.**, **Scully, M.E.**, **Traykovski, P.A.** and **Wheatcroft, R.A.** (2007) Sediment Delivery to the Seabed on Continental Margins. In: *Continental Margin Sedimentation: From Sediment Transport to Sequence Stratigraphy* (Eds C.A. Nittrouer, J.A. Austin, M.E. Field, J.H. Kravitz, J.P.M. Syvitski and P.L. Wiberg), IAS Spec. Publ., **37**, 49–99.

Howell, J.A., **Schwarz, E.**, **Spalletti, L.A.** and **Veiga, G.D.** (2005) The Neuquén Basin: an overview. In: *The Neuquén Basin, Argentina: A Case Study in Sequence Stratigraphy and Basin Dynamics* (Eds G. Veiga, L. Spalletti, J. Howell and E. Schwarz), Geol. Soc. London Spec. Publ., **252**, 1–14.

Kämpf, J. and **Myrow, P.** (2014) High-density mud suspensions and cross-shelf transport: on the mechanism of gelling ignition. *J. Sed. Res.*, **84**, 215–223.

Labaj, M.A. and **Pratt, B.R.** (2016) Depositional dynamics in a mixed carbonate-siliciclastic system: middle-upper Cambrian Abrigo Formation, Southeastern Arizona, U.S.A. *J. Sed. Res.*, **86**, 11–37.

Lazo, D.G. (2006) Análisis tafonómico e inferencia del grado de mezcla temporal y espacial de la macrofauna del Miembro Pilmatué de la Formacion Agrio, Cretácico Inferior de cuenca Neuquina, Argentina. *Ameghiniana*, **43**, 311–326.

Lazo, D.G. (2007) Análisis de biofacies y cambios relativos del nivel del mar en el Miembro Pilmatué de la Formación Agrio, Cretácico Inferior de cuenca Neuquina, Argentina. *Ameghiniana*, **44**, 73–89.

Legarreta, L. and **Gulisano, C.A.** (1989) Análisis estratigráfico secuencial de la Cuenca Neuquina (Triásico Superior-Terciario inferior). In: *Cuencas Sedimentarias Argentinas* (Eds G. Chebli and L.A. Spalletti), Serie Correlación Geológica, **6**, 221–243.

Legarreta, L. and **Uliana, M.A.** (1991) Jurassic-Cretaceous marine oscillations and geometry of a back-arc basin fill, central Argentine Andes. In: *Sedimentation, Tectonics and Eustacy. Sea Level Changes at Active Margins* (Ed. D.I.M. MacDonald), IAS Spec. Publ., **12**, 429–450.

Legarreta, L. and **Uliana, M.A.** (1999) El Jurásico y Cretácico de la Cordillera Principal y la Cuenca Neuquina. 1. Facies sedimentarias. In: *Geología Argentina* (Ed. R. Caminos), Instituto de Geología y Recursos Minerales. Servicio Geológico Minero Argentino, Anales, **29**, 399–416.

MacEachern, J.A., **Bann, K.L.**, **Pemberton, S.G.** and **Gingras, M.K.** (2007a) The ichnofacies paradigm: high-resolution paleoenvironmental interpretation of the rock record. In: *Applied Ichnology* (Eds J.A. McEachern, K.L. Bann, M.K. Gingras and S.G. Pemberton). SEPM Short Course Notes, **52**, 27–64.

MacEachern, J.A., **Pemberton, S.G.**, **Bann, K.L.** and **Gingras, M.K.** (2007b) Departures from the archetypal ichnofacies: effective recognition of physico-chemical stresses in the rock record. In: *Applied Ichnology* (Eds J.A. McEachern, K.L. Bann, M.K. Gingras and S.G. Pemberton). SEPM Short Course Notes, **52**, 65–93.

Madof, A.S., **Christie-Blick, N.** and **Anders, M.H.** (2015) Tectonically controlled nearshore deposition: cozzette Sandstone, Book Cliffs, Colorado, U.S.A. *J. Sed. Res.*, **85**, 459–488.

Michel, J., **Mateu-Vicens, G.** and **Westphal, H.** (2011) Modern heterozoan carbonate facies from a eutrophic tropical shelf (Mauritania). *J. Sed. Res.*, **81**, 641–655.

Morris, J.E., **Hampson, G.J.** and **Johnson, H.D.** (2006) A sequence stratigraphic model for an intensely

bioturbated shallow-marine sandstone: the Bridport Sand Formation, Wessex Basin, UK. *Sedimentology*, **53**, 1229–1263.

Mount, J.F. (1984) Mixing of siliciclastic and carbonate sediments in shallow shelf environments. *Geology*, **12**, 432–435.

Myrow, P.M. and **Southard, J.B.** (1996) Tempestite deposition. *J. Sed. Res.*, **66**, 875–887.

Naish, T.R. and **Kamp, P.J.J.** (1997) Sequence stratigraphy of sixth-order (41 k.y.) Pliocene-Pleistocene cyclothems, Wanganui basin, New Zealand: a case for the regressive systems tract. *Geol. Soc. Am. Bull.*, **109**, 978–999.

Nummedal, D. and **Swift, D.J.P.** (1987) Transgressive stratigraphy at sequence-bounding unconformities: some principles derived from Holocene and Cretaceous examples. In: *Sea-Level Fluctuation and Coastal Evolution* (Eds D. Nummedal, O.H. Pilkey and J.D. Howard), SEPM Spec. Publ., **41**, 241–260.

Parson, J.D., **Friedrichs, C.T.**, **Traykovski, P.A.**, **Mohrig, D.**, **Imran, J.**, **Syvitski, J.P.M.**, **Parker, G.**, **Puig, P.**, **Buttles, J.L.** and **García, M.H.** (2007) The mechanics of marine sediment gravity flows. In: *Continental Margin Sedimentation: From Sediment Transport to Sequence Stratigraphy* (Eds C.A. Nittrouer, J.A. Austin, M.E. Field, J.H. Kravitz, J.P.M. Syvitski and P.L. Wiberg), IAS Spec. Publ., **37**, 275–334.

Patterson, J.H. and **Henstridge, D.A.** (1990) Comparison of the mineralogy and geochemistry of the Kerosene Creek Member, Rundle and Stuart oil shale deposits, Queensland, Australia. *Chem. Geol.*, **82**, 319–339.

Patterson, J.H., **Hurst, H.J.**, **Levy, J.H.** and **Killingley, J.S.** (1990) Mineral reactions in the processing of Australian Tertiary oil shales. *Fuel*, **69**, 1119–1123.

Perillo, M.M., **Best, J.L.** and **García, M.H.** (2014) A new phase diagram for combined-flow bedforms. *J. Sed. Res.*, **84**, 301–313.

Pickerill, R.K. and **Brenchley, P.J.** (1991) Benthic macrofossils as paleoenvironmental indicators in marine siliciclastic facies. *Geosci. Can.*, **18**, 119–138.

Purdy, E.G. and **Gischler, E.** (2003) The Belize margin revisited. 1. Holocene marine facies. *Int. J. Earth Sci.*, **92**, 532–551.

Rankey, E.C. (2014) Contrasts between wave-and tide-dominated oolitic systems: holocene of Crooked-Acklins Platform, southern Bahamas. *Facies*, **60**, 405–428.

Reading, H.G. and **Collinson, J.D.** (1996) Clastic coasts. In: *Sedimentary Environments; Processes, Facies and Stratigraphy* (Ed. H.G. Reading), pp. 232–280. Blackwell Science, Oxford.

Sagasti, G. (2005) Hemipelagic record of orbitally-induced dilution cycles in Lower Cretaceous sediments of the Neuquén Basin. In: *The Neuquén Basin, Argentina: A Case Study in Sequence Stratigraphy and Basin Dynamics* (Eds G. Veiga, L. Spalletti, J. Howell and E. Schwarz), Geol. Soc. London Spec. Publ., **252**, 231–250.

Sanders, D. and **Höfling, R.** (2000) Carbonate deposition in mixed siliciclastic-carbonate environments on top of an orogenic wedge (Late Cretaceous, Northern Calcareous Alps, Austria). *Sed. Geol.*, **137**, 127–146.

Saul, G., **Naish, T.**, **Abbott, S.T.** and **Carter, R.M.** (1999) Sedimentary cyclicity in the marine Plio-Pleistocene: sequence stratigraphic motifs characteristic of the last 2.5 m.y. *Geol. Soc. Am. Bull.*, **111**, 524–537.

Scholle, P.A. and **Ulmer-Scholle, D.S.** (2003) *A Color Guide to the Petrography of Carbonate Rocks: Grains, Textures, Porosity, Diagenesis*. AAPG Mem., **77**, Tulsa, OK, 474 pp.

Schwarz, E. and **Howell, J.A.** (2005) Sedimentary evolution and depositional architecture of a Lowstand Sequence Set: Lower Cretaceous Mulichinco Formation, Neuquén Basin, Argentina. In: *The Neuquén Basin, Argentina: A Case Study in Sequence Stratigraphy and Basin Dynamics* (Eds G. Veiga, L. Spalletti, J. Howell and E. Schwarz). Geol. Soc. London Spec. Publ., **252**, 109–138.

Schwarz, E., **Spalletti, L.A.** and **Howell, J.A.** (2006) Sedimentary response to a tectonically-induced sea-level fall in a shallow back-arc basin: the Mulichinco Formation (Lower Cretaceous), Neuquén Basin, Argentina. *Sedimentology*, **53**, 55–81.

Schwarz, E., **Spalletti, L.A.**, **Veiga, G.D.** and **Fanning, M.** (2016a) First U-Pb SHRIMP Age for the Pilmatué Member (Agrio Formation) of the Neuquén Basin, Argentina: implications for the Hauterivian Lower Boundary. *Cretaceous Res.*, **58**, 223–233.

Schwarz, E., **Veiga, G.D.**, **Álvarez-Trentini, G.** and **Spalletti, L.A.** (2016b) Climatically versus eustatically controlled, sediment-supply-driven cycles: carbonate-siliciclastic, high-frequency sequences in the Valanginian of the Neuquén Basin (Argentina). *J. Sed. Res.*, **86**, 312–335.

Schwarz, E., **Echevarria, C.** and **Veiga, G.D.** (2016c) Caracterización paleoambiental y secuencial de depósitos deltaicos del Mb. Pilmatué en el centro de la Provincia de Neuquén (Argentina). In: *Abstracts Volume VII Congreso Latinoamericano de Sedimentología y XV Reunión Argentina de Sedimentología*, pp. 154. Santa Rosa, Argentina. ISBN: 978-987-42-2083-7.

Scotese, C.R. (2000) *The Paleomap Project*. Available at: http://www.scotese.com.

Spalletti, L.A., **Franzese, J.R.**, **Matheos, S.D.** and **Schwarz, E.** (2000) Sequence stratigraphy of a tidally dominated carbonate siliciclastic ramp; the Tithonian-Early Berriasian of the Southern Neuquén Basin, Argentina. *J. Geol. Soc. London*, **157**, 433–446.

Spalletti, L.A., **Poiré, D.G.**, **Pirrie, D.**, **Matheos, S.D.** and **Doyle, P.** (2001) Respuesta sedimentológica a cambios en el nivel de base en una secuencia mixta clástica-carbonática del Cretácico de la Cuenca Neuquina, Argentina. *Rev. Soc. Geol. Esp.*, **14**, 57–74.

Spalletti, L.A., **Veiga, G.D.**, **Schwarz, E.** and **Franzese, J.F.** (2008) Depósitos de flujos gravitacionales subácueos de sedimentos en el flanco activo de la Cuenca Neuquina durante el Cretácico Temprano. *Rev. Asoc. Geol. Argentina*, **63**, 442–453.

Spalletti, L.A., **Veiga, G.D.** and **Schwarz, E.** (2011) La Formación Agrio (Cretácico Temprano) en la Cuenca Neuquina. In: *Geología y Recursos Naturales de la Provincia del Neuquén* (Eds H. Leanza, J. Vallés, C. Arregui and J. C Danieli), pp. 145–160. Relatorio del XVIII Congreso Geológico Argentino, Buenos Aires.

Swift, D.J.P., **Phillips, S.** and **Thorne, J.A.** (1991) Sedimentation on continental margins: V. Parasequences. In: *Shelf Sand and Sandstone Bodies; Geometry, Facies and Sequence Stratigraphy* (Eds D.J.P. Swift, G.F. Oertel, R.W. Tillman and J.A. Thorne), IAS Spec. Publ., **14**, 153–187.

Taylor, A.M. and **Goldring, R.** (1993) Description and analysis of bioturbation and ichnofabric. *J. Geol. Soc. London*, **150**, 141–148.

Van Siclen, D.C. (1964) Depositional topography in relation to cyclic sedimentation. In: *Symposium on Cyclic*

Sedimentation (Ed. D.F. Merriam), Kansas Geological Survey, Bulletin **169**, 533–539.

Van Wagoner, J.C., **Posamentier, H.W.**, **Mitchum, R.M.**, **Vail, P.R.**, **Sarg, J.F.**, **Loutit, T.S.** and **Hardenbol, J.** (1988) An overview of the fundamentals of sequence stratigraphy and key definitions. In: *Sea-Level Change: An Integrated Approach* (Eds C.K. Wilgus, B.J. Hastings, H. Posamentier, J.C. Van Wagoner, C.A. Ross and C.G.St.C. Kendall), SEPM Spec. Publ., **42**, 39–46.

Van Wagoner, J.C., **Mitchum, R.M.**, **Campion, K.M.** and **Rahmanian, V.D.** (1990) *Siliciclastic Sequence Stratigraphy in Well Logs, Cores, and Outcrop: Concepts for High-Resolution Correlation of Time and Facies*. AAPG, Methods in Exploration Series, **7**, Tulsa, OK, 255 pp.

Veiga, G.D. and **Schwarz, E.** (2017) Facies characterization and sequential evolution of an ancient offshore dunefield in a semi-enclosed sea: Neuquén Basin, Argentina. *Geo-Mar. Lett.*, **37**, 411–426.

Veiga, G.D., **Spalletti, L.A.** and **Flint, S.** (2002) Aeolian/fluvial interactions and high resolution sequence stratigraphy of a non-marine lowstand wedge: the Avilé Member of the Agrio Formation (Lower Cretaceous) in central Neuquén Basin, Argentina. *Sedimentology*, **49**, 1001–1019.

Veiga, G.D., **Spalletti, L.A.** and **Flint, S.S.** (2007) Anatomy of a fluvial lowstand wedge: the Avilé Member of the Agrio Formation (Hauterivian) in central Neuquén Basin (northwest Neuquén province), Argentina. In: *Sedimentary Environments, Processes and Basins. A Tribute to Peter Friend* (Eds G. Nichols, E. Williams and C. Paola), IAS Spec. Publ., **38**, 341–365.

Vital, H., **Stattegger, K.**, **Amaro, V.E.**, **Schwarzer, K.**, **Frazão, E.P.** and **Tabosa, W.F.A.** (2008) Modern high-energy siliciclastic-carbonate platform: Continental shelf adjacent to Northern Rio Grande do Norte State, NE Brazil. In: *Recent Advances in Models of Siliciclastic Shallow-Marine Stratigraphy* (Eds G. Hampson, R. Steel, P. Burgess and R. Dalrymple), SEPM Spec. Publ., **90**, 177–190.

Walker, R.G. and **Plint, A.G.** (1992) Wave- and storm-dominated shallow marine systems. In: *Facies Models: Response to Sea Level Change* (Eds R.G. Walker and N.P. James), Geol. Assoc. Can., Geotext **1**, 219–238.

Weaver, V. (1931) Palaeontology of the Jurassic and Cretaceous of West Central Argentina. *Memoirs Univ. Washington*, **1**, 1–595.

Zecchin, M. and **Catuneanu, O.** (2013) High-resolution sequence stratigraphy of clastic shelves I: units and bounding surfaces. *Mar. Petrol. Geol.*, **39**, 1–25.

Zecchin, M., **Catuneanu, O.** and **Caffau, M.** (2017) High-resolution sequence stratigraphy of clastic shelves V: Criteria to discriminate between stratigraphic sequences and sedimentological cycles. *Mar. Petrol. Geol.*, **85**, 259–271.

Zeller, M., **Verwer, K.**, **Eberli, G.P.**, **Massaferro, J.L.**, **Schwarz, E.** and **Spalletti, L.** (2015) Depositional controls on mixed carbonate–siliciclastic cycles and sequences on gently inclined shelf profiles. *Sedimentology*, **62**, 2009–2037.

Zonneveld, J.P., **Gingras, M.K.** and **Pemberton, S.G.** (2001) Trace fossil assemblages in a Middle Triassic mixed siliciclastic-carbonate marginal marine depositional system, British Columbia. *Palaeogeogr. Palaeoclimatol. Palaeoecol.*, **166**, 249–276.

Manuscript received 25 April 2017; revision accepted 1 November 2017